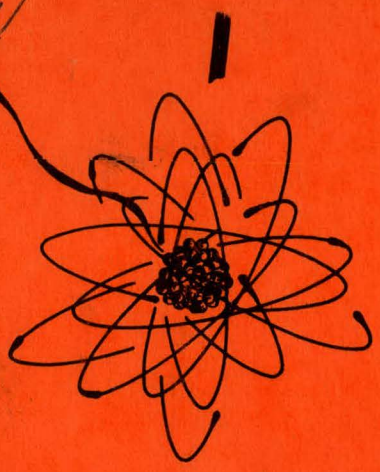

YAEC-80

YANKEE ATOMIC ELECTRIC COMPANY

RESEARCH AND DEVELOPMENT PROGRAM

THERMAL DEFLECTION OF THE YANKEE FUEL ASSEMBLY FROM LINEAR AND NON-LINEAR TEMPERATURE GRADIENTS

R&D SUBCONTRACT NO. 1 under

USAEC - YAEC CONTRACT AT (30-3)-222

MARCH, 1959

WESTINGHOUSE ELECTRIC CORPORATION

ATOMIC POWER DEPARTMENT

PITTSBURGH,30 P. O. BOX 355 PENNSYLVANIA

DISCLAIMER

YAEC-80

Yankee Atomic Electric Company

Research And Development Program

THERMAL DEFLECTION OF THE YANKEE FUEL ASSEMBLY FROM LINEAR AND NON-LINEAR TEMPERATURE GRADIENTS

by

Carl G. Johnson
Thermal, Hydraulic and Mechanical Design
Section

March, 1959

For The Yankee Atomic Electric Company
Under Research and Development Subcontract
No. 1 of USAEC-YAEC Contract AT(30-3)-222

APPROVED:

W. E. Abbott, Manager
Reactor Development
Department

Westinghouse
ELECTRIC CORPORATION
ATOMIC POWER DEPARTMENT
P.O. BOX 355
PITTSBURGH 30, PA.

EXTERNAL DISTRIBUTION

USAEC, New York Operations Office - 70 Columbus Avenue, New York 23, N. Y.	4
USAEC, Division of Reactor Development - 1717 H Street, Washington 25, D. C.	8
USAEC, Commissioner Patent Branch - Washington 25, D. C.	1
USAEC, Technical Information Service Ext. - P.O. Box 62, Oak Ridge, Tennessee	20
Yankee Atomic Electric Company - 441 Stuart Street, Boston 16, Massachusetts	22
W. J. Miller - Yankee Atomic Electric Company Representative 453 Market Street, Beaver, Pennsylvania	1
TOTAL	56

Standard distribution to be made by TISE, Oak Ridge, Tennessee under Category - "Reactors - Power," as provided in the current edition of TID-4500.

WESTINGHOUSE DISTRIBUTION

R. L. Wells - W. E. Shoupp	1	A. B. Holt	1
H. C. Amtsberg - R. W. Garbe	1	H. A. Smith	1
W. E. Johnson	1	C. F. Obermesser	1
A. E. Voysey	1	J. J. Loving	1
H. E. Walchli	4	E. A. Goldsmith	1
G. M. Inman	1	P. B. Haga	1
H. L. Russo	1	W. K. Stromquist	1
H. W. P. Stanhope	1	J. F. Chalupa	1
A. R. Del Campo	1	D. G. Brunstetter	1
E. U. Powell	1	J. J. Lombardo	1
S. M. Marshall	1	W. E. Abbott	1
A. R. Jones	2	I. H. Coen	1
T. Stern	1	A. G. Thorp II	1
R. L. Stoker	1	P. W. Davison	2
W. L. Budge	1	H. W. Graves, Jr.	1
E. T. Morris - M. A. Schultz	1	W. H. Arnold	1
H. J. Garber	1	G. H. Minton	1
J. C. Danko	1	A. J. Dolan - New York	1
D. H. Fax	1	H. P. Turner - Boston	1
Technical Information Center	2		
		TOTAL	45

TABLE OF CONTENTS

Page

LIST OF FIGURES

List of Figures (cont'd)

LIST OF TABLES

I. ABSTRACT

Theoretical conditions have been investigated for determining the thermal deflection of the definitive design unshrouded Yankee fuel assembly and the compromise design fuel assembly. In addition, an experimental study has been completed on the thermal deflection of the compromise design fuel assembly from linear and non-linear temperature gradients.

All of the theoretical analyses performed on the definitive design clearly indicate that excessive bowing in the order of 0.150 inch may occur within the reactor during normal operation. Since the nominal clearance available in this design between a fuel assembly and an adjacent control rod is about 0.120 inch, interference between a fuel assembly and its adjacent control rod can occur, resulting in restricting the movement of the control rod. When buildup of mechanical tolerances are considered, this condition becomes more severe. Redesign of the definitive design fuel assembly thus became mandatory to prevent interference with the movement of control rods. The compromise fuel assembly design evolved as a result of these considerations.

The compromise design employs the use of the brazed ferrule fuel sub-assembly design concept, but incorporates several fundamental changes in design that increase clearances adjacent to the control rod to reduce thermal bowing of the complete assembly. The compromise fuel assembly is allowed to deflect under thermal distortion to a limited extent and is designed so that under the worst set of circumstances the available clearance between the fuel assembly and control rod is at least 0.001 inch. The compromise design therefore, constitutes a safe design from a thermal deflection standpoint.

II. INTRODUCTION

In the Yankee pressurized light-water reactor, each fuel assembly is made up of several individual, unshrouded fuel subassemblies that consist of a geometrical array of stainless steel tubes which contain uranium fuel in the form of a ceramic pellet. The tubes are joined together by means of brazed ferrules in layers of various configurations spaced along the longitudinal axis as illustrated in Figure 1. Control of the nuclear reaction is provided by unshrouded cruciform control rods which are spaced between fuel assemblies. Since both fuel assemblies and control rods are unshrouded along their entire length, surface contact between a fuel bundle and an adjacent control rod can occur.

Because of the inherent mechanical design of the fuel assembly, each subassembly can act essentially independent of the other subassemblies within the fuel assembly; that is to say, each subassembly can deflect in any radial direction about its own neutral axis without considering its effect on the other subassemblies. This basic assumption is made so that a subassembly can be analyzed as a separate entity within the reactor and is not limited by any appreciable end moment and shear that may be transmitted through the end nozzle to the other subassemblies. Therefore, this analysis applies to a single subassembly within a complete fuel assembly.

When the reactor is in operation, a condition may exist in which a row of tubes on one side of a subassembly may be located in an average thermal channel for that location in the reactor while the other opposite row of tubes may be located in a hot channel. Since the thermal design of a reactor imposes the limitation of applying hot channel factors in the heat transfer analysis, it is both reasonable and conservative to assume that the mechanical design should be subject to the same qualifications. Accordingly, engineering hot channel factors are applied to the row of tubes located in the hot channel. In addition to these factors, a radial variation in power density across a subassembly due to nuclear characteristics must be considered. Flux peaking in the vicinity of a control rod or follower enters the analysis as a separate factor. When all of the above factors are grouped so as to be additive, a condition which may often occur within the reactor, a temperature gradient of linear or non-linear character is induced across the subassembly causing it to deflect or bow. Excessive bowing becomes a definite possibility when the temperature gradient is large. Interference with the moment of a control rod by a deflected definitive design fuel assembly becomes likely during normal operation when the thermal deflection is added to the mechanical tolerance buildup. The locking force holding the control rod in a fixed position may be of sufficient magnitude to prevent the control rod from moving within the core. When scramming becomes necessary the situation may become critical because it may mean that control of the reactor has been lost. It may be concluded, therefore, that accurate computation of thermal deflection of a subassembly according to best engineering knowledge is a necessary and vital analysis that should be performed on any reactor.

Unfortunately, very little information has been published on the subject of the thermal deflection of reactor fuel assemblies. Present knowledge indicates that there has been no publication to date that contains an analysis of the thermal deflection of fuel assemblies as applied to tubular bundles of fuel rods.

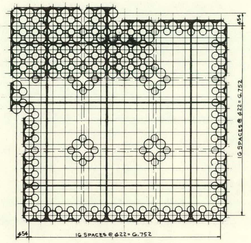

SECTION B-B

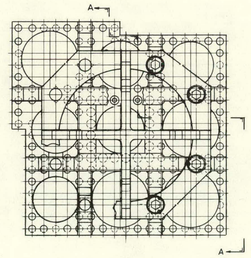

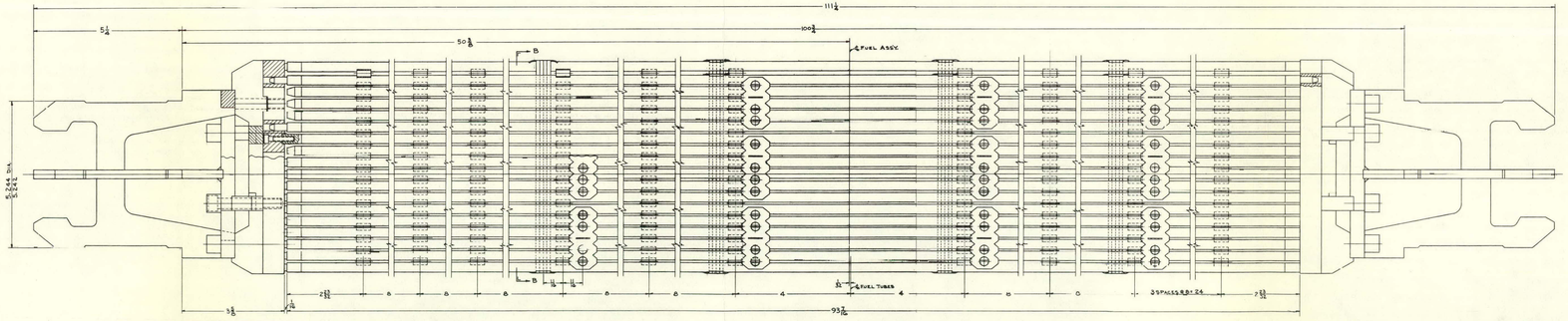

SECTION A-A

FIGURE 1

TITLE COMPROMISE FUEL ASSEMBLY								
DWG. 646J642								
PLAN 1								
	DESCRIPTION & MATERIAL DIMENSIONS IN INCHES	PLATE MFR. REF. DWG.	PCS. PER ASSY.	STYLE NO.				

WESTINGHOUSE ELECTRIC CORPORATION

TITLE LARGE PRESSURIZED WATER NUCLEAR POWER PLANT - COMPROMISE FUEL ASSEMBLY

DIMENSIONS IN INCHES SCALE NTS

MFR. 'C' SHEET	DES. APPR.		646J642
	APPR.		
CHKD.	APPR.		

DIV. & PLANT LOCATION ATOMIC POWER DEPT.

III. CONCLUSIONS

The compromise fuel assembly design is recommended for use in the Yankee Reactor in order to eliminate the problem of excessive thermal deflection. The design, shown in Figure 1, consists of eight subassemblies which float freely in the axial direction and surround a ninth rigid center subassembly fixed securely to a new type of handling socket. The eight outer floating assemblies are guided on each end by extruded end plugs in the handling sockets and are tied integrally together at various axial stations by thin straps such that all subassemblies must bow the same amount. This arrangement results in minimizing thermal bowing since the subassemblies which do not experience high thermal gradients act to restrain the remaining subassemblies.

As a result of the theoretical and experimental analyses performed, the numerical summation method derived in this report for predicting the center deflection of a reactor fuel subassembly is the procedure that should be followed in analyzing thermal deflection. A reactor fuel subassembly of the hollow tube type cannot be approximated by a solid rectangular beam to determine thermal deflection from non-linear temperature gradients. Only in the specialized case, where the temperature gradient is linear throughout, can the solid beam theory be applied. The numerical summation method yields thermal deflections which are within $\pm$ 5% of the actual experimental values and constitutes an excellent method for obtaining thermal deflections.

IV. NOMENCLATURE

A	- Area of fuel subassembly cross section, $in.^2$
A_s	- Surface area in x increment of fuel tube, $in.^2$
a,b,c	- Constants
α	- Coefficient of thermal expansion, in./in.-°F
b_1	- Outside radius of fuel tube, in.
c	- Half height of beam, in.
C_p	- Specific heat of water at average temperature in channel, °F
C_1, C_2	- Constants
γ_{xy}	- Unit shearing strain, in./in.
Δ	- Deflection of subassembly, in.
Δ_{max}	- Maximum thermal deflection, in.
Δ_E	- Extrapolated deflection for 50°F differential, in.
Δ_{test}	- Thermal deflection from experimental test, in.
e	- Base of natural logarithms, dimensionless
$\varepsilon_x, \varepsilon_y, \varepsilon_z$	- Unit normal strains, in./in.
E	- Young's Modulus, psi
$\bar{e},d,g,h$	- Constants
$F_{\Delta T}$	- Coolant water hot channel factor, dimensionless
F_{fp}	- Flux peaking hot channel factor, dimensionless
F_θ	- Film temperature hot channel factor, dimensionless
F_q	- Heat flux hot channel factor, dimensionless
F	- Tensile force, lbs.
$F(x)$	- Functions of x only
$G(y)$	- Functions of y only

NOMENCLATURE

h_F	- Heat transfer film coefficient, Btu/hr-ft^2-°F
I	- Moment of inertia of sub-assembly, in.^{4}
k	- Thermal conductivity of tube, Btu/hr-ft^2-°F-ft
K	- Function independent of x and y
L	- Half length of subassembly, in.
ΔL	- Change in length of subassembly, in.
M	- Experimental end moment, lb-in.
N	- Number of rods, dimensionless
P	- Experimental end moment load, lbs.
Q	- Total heat output of reactor, Btu/hr.
$\overline{Q}$	- Average heat output per rod, Btu/hr-rod
Q_x	- Heat output in x increment, Btu/hr
ν	- Poisson's ratio, dimensionless
R	- Radius of curvature of deflected subassembly, in.
$\sigma_x, \sigma_y, \sigma_z$	- Unit normal stress, psi
Σ	- Summation function
T_{w_x}	- Water temperature at x location, °F
T_{s_x}	- Surface temperature at x location, °F
T_{c_x}	- Tube (clad) temperature at x location, °F
$\overline{T}_o$	- Average inlet coolant temperature, °F
T_o	- Constant coefficient, dimensionless
$T_{s_{avg}}$	- Average surface temperature in channel, °F
$T_{c_{avg}}$	- Average tube (clad) temperature in channel, °F

NOMENCLATURE

$T_{c_{\text{Hot Channel}}}$	- Average tube (clad) temperature in hot channel, °F
$T(y)$	- Temperature function of y
τ_{xy}	- Unit shearing stress, psi
ΔT_{w_x}	- Temperature rise of water in x increment, °F
ΔT_{c_x}	- Temperature rise in tube (clad) wall, °F
$\Delta T_{w_{H.C.}}$	- Temperature rise of water in hot channel, °F
$\Delta T_{c_{H.C.}}$	- Temperature rise of tube in hot channel, °F
$\overline{\Delta T_c}$	- Average mean tube temperature difference for non-linear thermal gradient, °F
θ	- One-half the angle subtended by an arc with radius of curvature R, radius
$\theta_{F_{H.C.}}$	- Film temperature rise in hot channel, °F
θ_{F_x}	- Film temperature rise in x increment, °F
μ	- Displacement in x direction, in.
ν	- Displacement in y direction, in.
W	- Mass flow rate for heat transfer analysis, lbs/hr
x, y, z	- Principal directions
y	- Distance, in.
T_{in}	- Coolant inlet temperature, °F

V. STATEMENT OF PROBLEM

The purpose of the present investigation is to obtain a solution for the thermal deflection of a tubular type reactor fuel subassembly under linear and non-linear temperature gradients. A procedure is described which illustrates the method of obtaining a linear and a non-linear temperature distribution across a fuel subassembly as a result of reactor analysis. The problem of thermal deflection resulting from a linear temperature gradient is solved by two independent methods presented in the following section. In the non-linear temperature distribution case, experimental results are presented which demonstrate that the tubular subassembly cannot be treated as a beam. A numerical integration method is presented which accurately predicts thermal deflections for the non-linear case to within experimental error. The derivations of all equations are included within the body of the text.

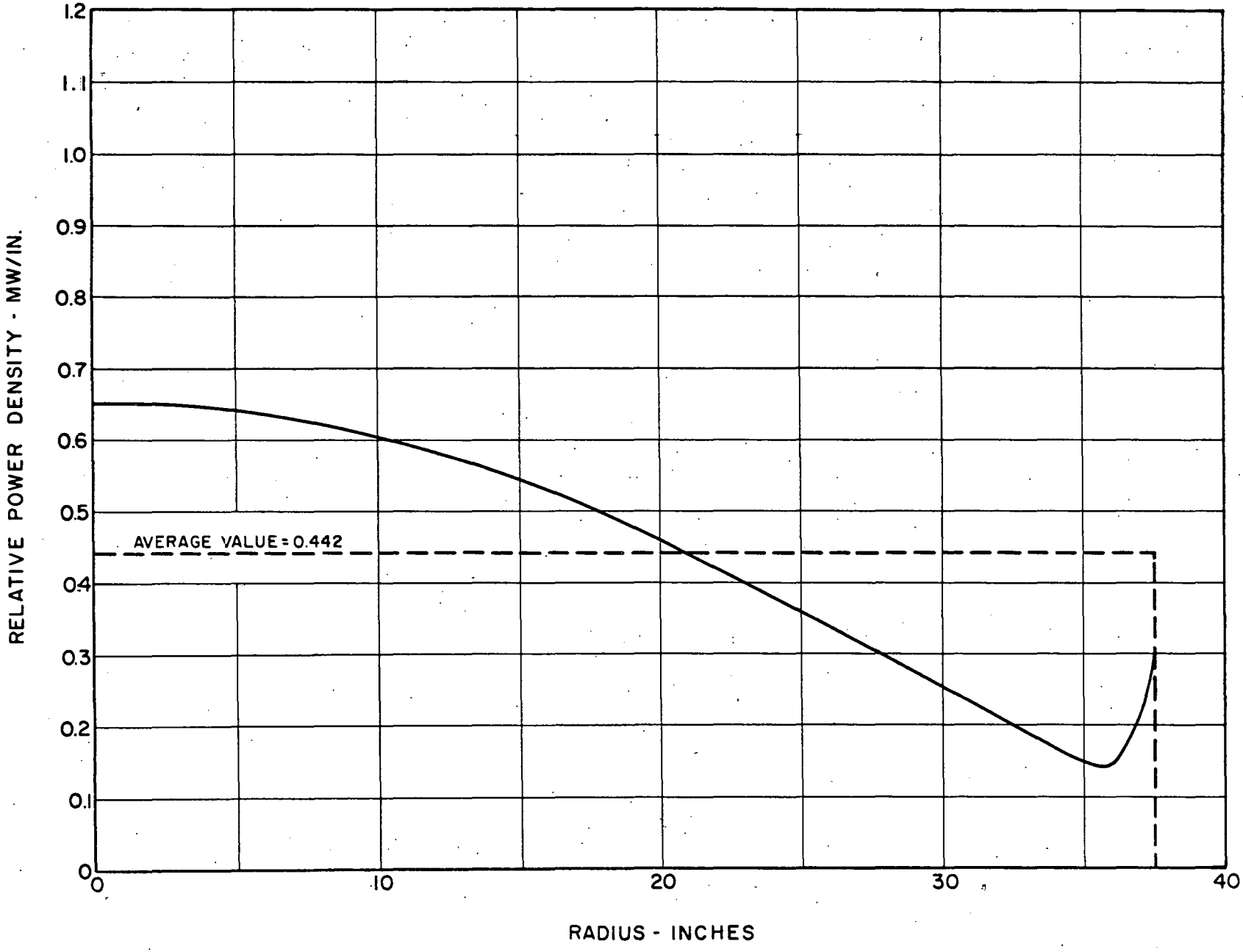

FIGURE 2 RADIAL POWER CURVE FOR TYPICAL REACTOR WITH CORE OF A UNIFORM ENRICHMENT OF 3.15%

VI. ANALYSIS

The heat transfer analysis involves calculating the temperature rise of the bulk water as it passes through the core and determining the axial variation in surface temperature and clad (tube) temperature for both the row of tubes in the average or nominal channel and for the row of tubes in the hot channel with flux peaking factors applied. By calculating the mean clad temperature verus distance through the core for both cases, the respective curves of temperature versus distance can be constructed and graphically integrated with a planimeter to obtain the average mean clad temperature. The difference between the average mean clad temperature for the tube row in the hot channel and that in the average channel determines the thermal gradient across the fuel subassembly cross-section. In the linear case, this is merely the difference between the average mean clad temperature on the opposite sides of the subassembly. In the non-linear case, the thermal gradient is taken between two adjacent rows of tubes and all of the gradients are summed to yield the total non-linear variation across the subassembly.

In order to analyze the effect of radial and axial variations in power density (or heat output), a nuclear analysis of the core parameters must be performed to produce radial and axial power density plots. The radial and axial power density plots for the uniform and two-region cores investigated herein, were furnished from computer results. Figures 2, 3 and 4 are included to demonstrate typical results of such an investigation. The relative radial power density curve of Figure 2 based on uniform isotopic enrichment of 3.15% yields a power density maximum-to-average ratio of 1.87.

In some cases, this radial power gradient may be considered too high, so the core may be loaded with two different enrichments to flatten the radial power curve. Figure 3 illustrates a two region core with a maximum-to-average power ratio of 1.28. The axial relative power density curve, Figure 4 may be used in combination with either the uniformly enriched core or the two region core since it is independently derived and has a power density maximum-to-average ratio of 2.00. All such nuclear plots are based upon a homogenized region of core converted from the actual square geometry to cylindrical co-ordinates. The analysis involving temperature determinations is therefore subject to the inherent nuclear limitations.

A. Equations Defining Temperature Rise

Consider the total thermal heat output of a reactor to be Q. By dividing the total heat output Q by the total number of rods N, the average heat output per rod, $\bar{Q}$, is determined. The total heat output of 392 megawatts in the Yankee Reactor is uniformly divided by the total number of rods to yield an average heat output per rod of 57,700 Btu/hr-rod. The subassembly within a fuel assembly is selected for analysis at a given equivalent radius depending upon its location in the core. The average heat output per rod $\bar{Q}$, is multiplied by the ratio of local-to-average power density to obtain the heat output in that rod or row of rods at that radial location in the core. One side of a subassembly will therefore have a different heat output than the other side, or considering each row of tubes in a subassembly, each row will have a different heat output.

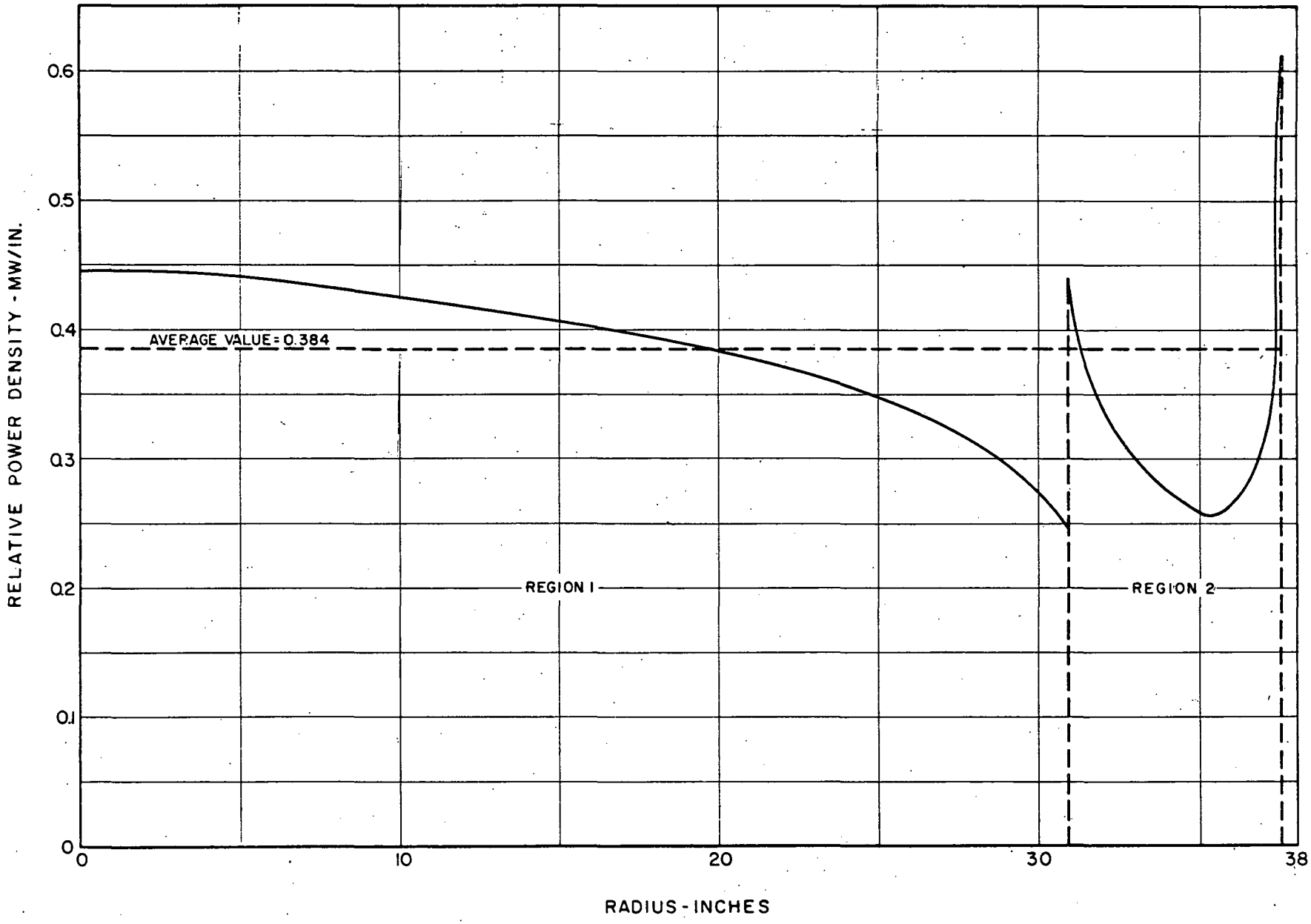

FIGURE 3 RADIAL POWER CURVE FOR TYPICAL REACTOR WITH CORE OF A TWO REGION LOADING

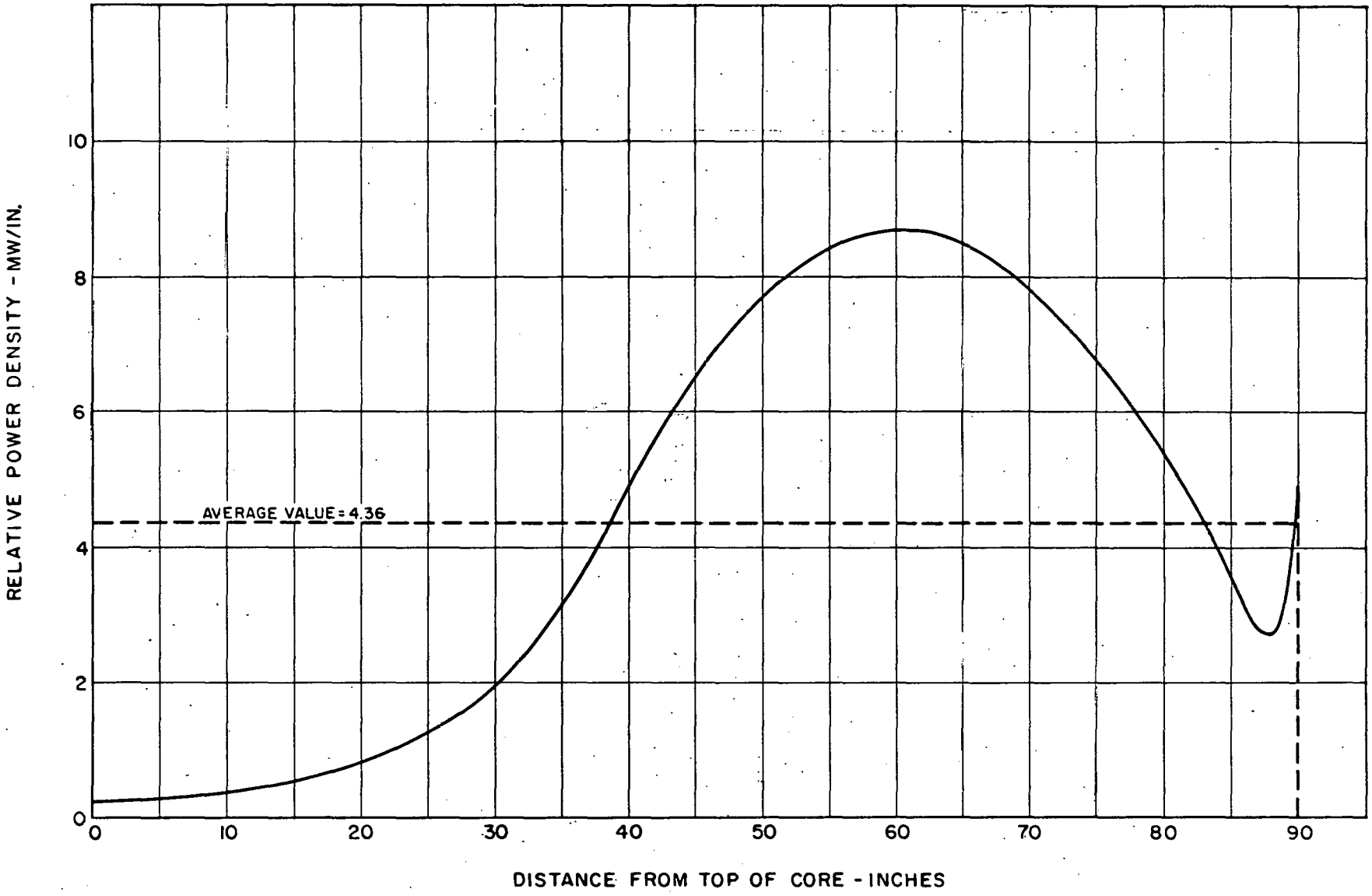

FIGURE 4 AXIAL POWER CURVE FOR TYPICAL REACTOR WITH CORE CONTROL RODS IN TO DEPTH EQUIVALENT TO AXIAL $\frac{\text{max.}}{\text{avg.}}$ POWER = 2 DISTANCE IN FROM TOP OF CORE = 36.6 INCHES

Knowing the heat output in a rod at a particular radius in the core, the general heat transfer analysis may be applied.

The axial core distance of 2L length may be conveniently divided into equal increments of x units each. From the axial power density plot, Figure 4, the percentage heat given off in that increment can be computed specifically from the total heat output in that channel. The temperature rise of the water in each increment is computed as follows:

$$Q_x = W C_p \Delta T_{w_x} \tag{1}$$

where the subscript x refers to the increment along the core being considered. The W factor is the mass flow rate based on the coolant flow heat transfer rate divided by the total number of rods N. The specific heat, C_p, is estimated based on the average temperature of the bulk water in the channel. For purposes of illustration, the inlet bulk water temperature to the core may be assumed as $\overline{T}_o$ in all cases, so that the temperature of the water in any increment is:

$$T_{w_x} = \overline{T}_o + \sum_{1}^{N} \Delta T_{w_N} \tag{2}$$

Now the film temperature rise must be calculated so the surface temperature can be obtained. The equation defining film temperature rise is given as:

$$Q_x = h_f \cdot A_s \cdot \theta f_x \tag{3}$$

where h_f, the average heat transfer film coefficient for pressurized water reactors is approximately 6000 Btu/hr-ft^2-°F and the surface area A_s is the outside area of a fuel tube in the x increment. The final surface temperature at each point is obtained from:

$$T_{s_x} = T_{w_x} + \theta f_x \tag{4}$$

The mean clad (tube) temperature must be determined by considering the temperature rise through the clad and applying the Fourier conduction law $q = -KA \frac{dT}{dr}$ which, developed in appropriate fashion, is:

$$\Delta T_{c_x} = \frac{Q_x \ln \frac{b_1}{a_1}}{2\pi KL} \tag{5}$$

for a hollow circular cylinder, where b_1 is the outside radius and a_1 is the inside radius. The arithmetic mean temperature of the clad is next computed from the relation:

$$T_c = T_{s_x} + \frac{\Delta T_{c_x}}{2} \tag{6}$$

The logarithmetic mean temperature is not used because the percentage error from the arithmetic mean temperature is small, i.e. less than 1%. The surface temperature and mean clad temperature pattern versus distance through the core may now be plotted and an average surface and clad temperature can be determined from the following:

$$T_{s_{avg}} = \frac{\int_o^y f\,(T_s)\,dy}{\int_o^y dy} \tag{7a}$$

$$T_{c_{avg}} = \frac{\int_o^y f\,(T_c)\,dy}{\int_o^y dy} \tag{7b}$$

A typical plot of this temperature variation is shown in Figure 5 for an average channel.

In order to compute the temperature rise of water in the hot channel, the actual ΔT_w in equation (1) must be multiplied by the hot channel and flux peaking factors. The formulas given below apply to the hot channel:

For the water temperature rise:

$$\Delta T_{w_{H.C.}} = F_{\Delta T} \cdot F_{fp} \cdot \Delta T_{w_x} \tag{8}$$

For the film temperature rise:

$$\theta_{f_{H.C.}} = F_{\theta} \cdot F_{fp} \cdot \theta_{f_x} \tag{9}$$

For the clad temperature rise:

$$\Delta T_c = F_q \cdot F_{fp} \cdot \Delta T_{c_x} \tag{10}$$

A typical plot of this hot channel temperature variation is shown in Figure 6.

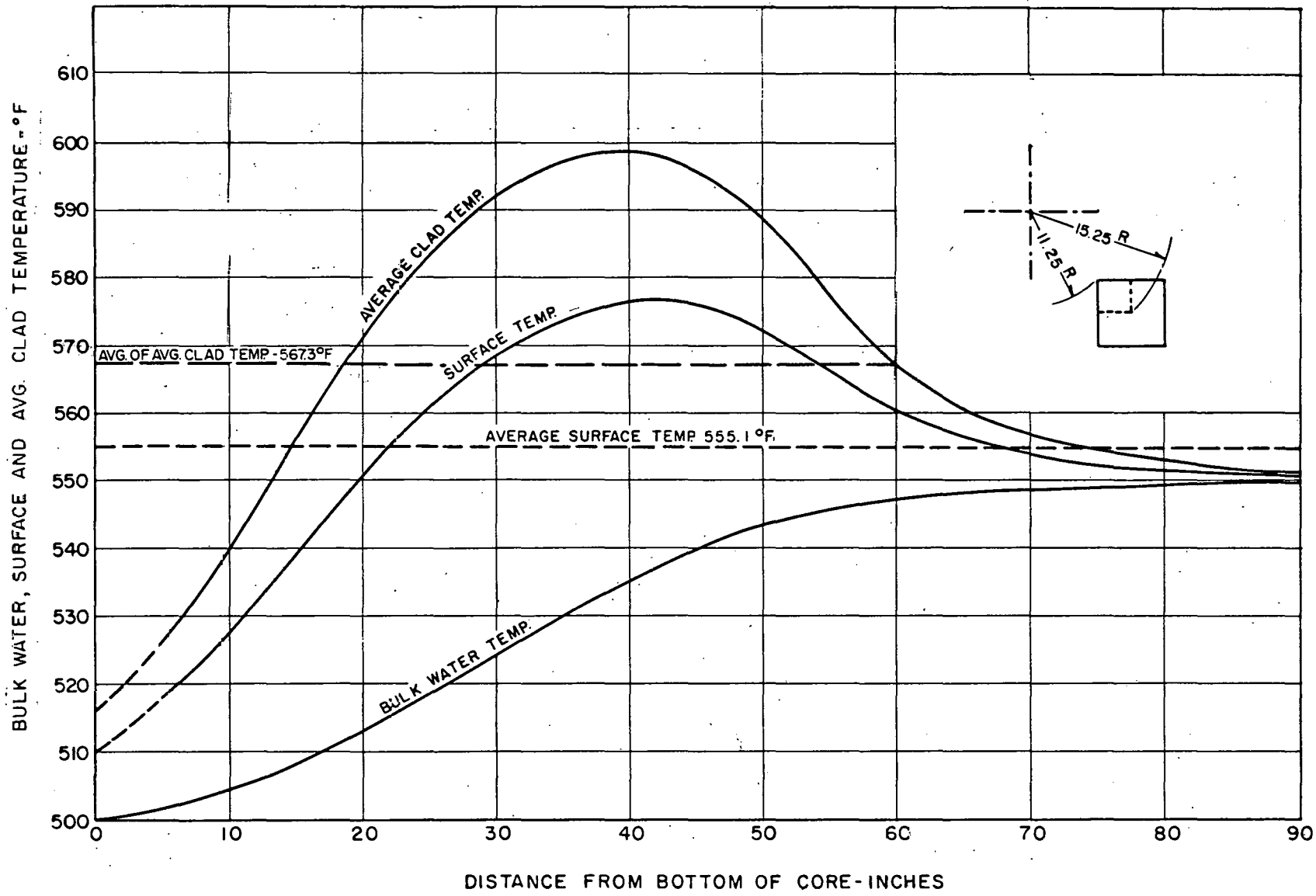

FIGURE 5 BULK WATER, SURFACE, AND AVG. CLAD TEMPERATURE VERSUS DISTANCE THROUGH CORE FOR TYPICAL ROD LOCATED AT 15.25 INCHES EQUIVALENT RADIUS IN AVERAGE CHANNEL FOR TYPICAL REACTOR.

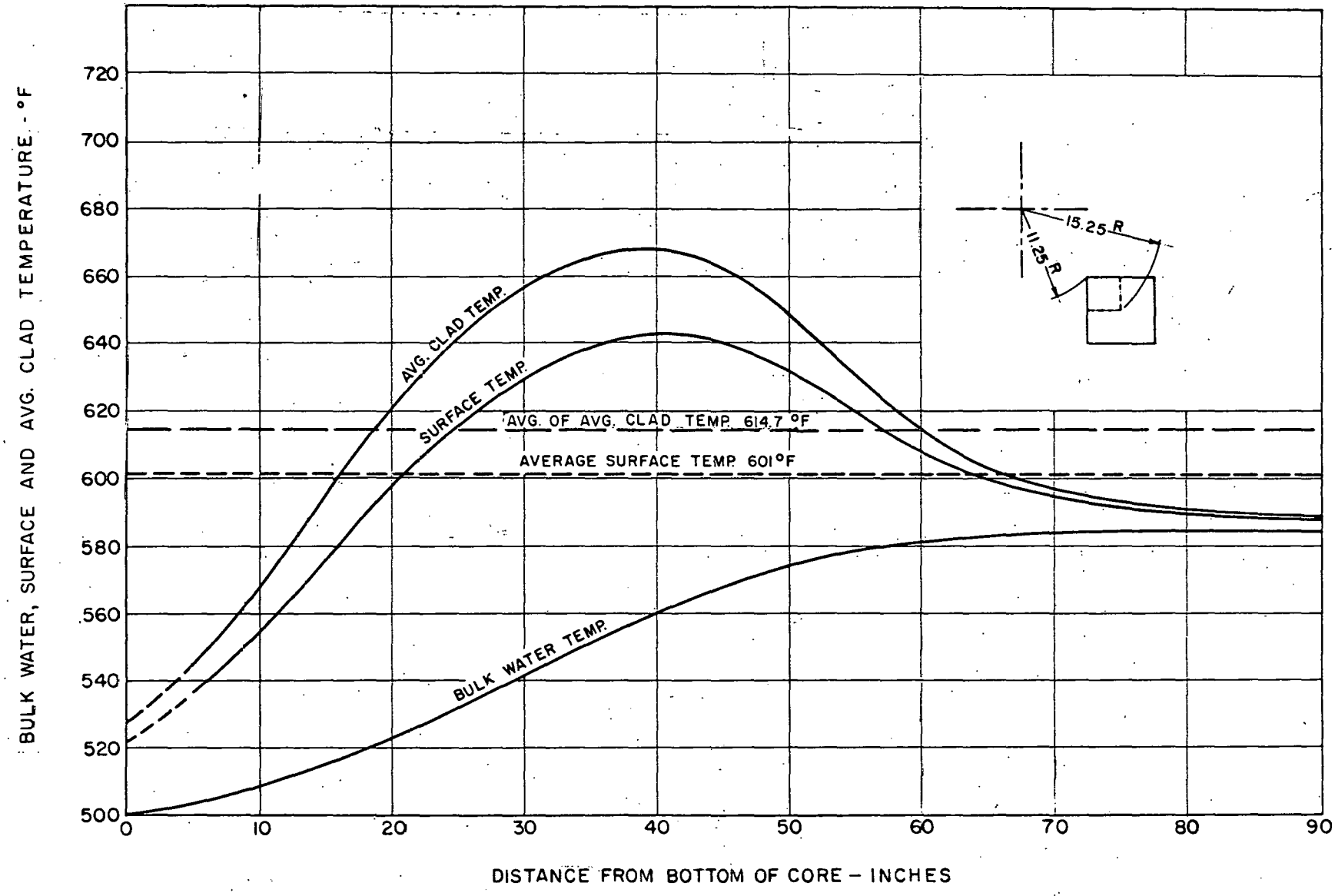

FIGURE 6 BULK WATER, SURFACE AND AVG. CLAD TEMPERATURE VERSUS DISTANCE THROUGH CORE FOR TYPICAL ROD LOCATED AT 11.5 INCHES EQUIVALENT RADIUS IN HOT CHANNEL FOR TYPICAL REACTOR.

The average mean clad temperature difference across the subassembly cross section for the linear case is:

$$\overline{\Delta T}_c = T_{c\ \text{Hot channel}} - T_{c\ \text{Avg. channel}} \qquad (11)$$

whereas the average mean clad temperature variation across adjacent tubes of the subassembly for the non-linear case is:

$$\overline{\Delta T}_{c_{N.L.}} = \frac{1}{N} \sum_{1}^{N} \left(T_{c\ \text{Hot channel}}^{N} - T_{c_{\text{Avg. channel}}}^{N+1} \right) \qquad (12)$$

B. Heat Transfer Method of Analysis

The heat transfer method of analysis is essentially similar to that used in the thermal design of the reactor and hot channel factors determined from thermal design considerations are used herein. Therefore, for the Yankee reactor, the coolant flow factor $F_{\Delta T}$ was considered as being equal to 1.392, the film factor F_θ, as 1.532 and the heat flux factor F_q as 1.078. Flux peaking factors, F_{fp} are taken as 1.20 and 1.38 for a center traverse and diagonal traverse, respectively, through a unit cell. The heat transfer analysis is accomplished by applying the formulas given in the previous section, thereby determining the average mean clad temperature difference.

C. Core Types Investigated

The maximum thermal deflection will depend upon the core type under consideration. Figure 2 shows the relative radial power density of a reactor core with a uniform enrichment of 3.15% and, although the maximum-to-average power density radially is high at 1.87, this type of loading in a homogeneous core will not yield the largest thermal gradient across a subassembly. The two region core, Figure 3, yields a somewhat greater thermal gradient since the slope of the power density curve in the outer region is the maximum for a given subassembly. However, other conditions must be considered in the analysis in addition to the maximum thermal gradient to achieve the maximum thermal deflection of a subassembly. It can be concluded that the relative position selected for analysis of thermal deflections is of prime importance.

1. Position in Core

Since it is very difficult to determine the position of the subassembly in both cores that will yield the greatest thermal gradient, several random positions have been selected and investigated. Table I shows the positions investigated in each core for the definitive design, the maximum thermal gradient resulting, the factors in the analysis that applied and the effective bowing of the assembly. Bowing computations were made only when the maximum clad temperature difference proved to be over 30°F.

TABLE I

Summary of Bowing Computations - Yankee Definitive First Core

Analysis No.	Core Type	Type of Traverse	Inner Tubes Located at Radius of (in.)	$F_{\Delta T}$*	F_{θ}*	F_{fp}*	F_{q}*	Outer Tubes Located at Radius of (in)	ΔT_c °F	Avg. Bowing in.	Avg. Bowing in.
Prelim.	Uniform	Diagonal	22.4	1.0	1.0	1.0	1.0	27.4	10.6	-	-
1	Uniform	Diagonal	22.4	1.392	1.532	1.0	1.078	27.4	32.2	0.061	0.070
2	Uniform	Diagonal	0.5	1.392	1.532	1.0	1.078	5.50	28.8	-	-
3	Uniform	Center	11.5	1.392	1.532	1.20	1.078	15.25	47.4	0.127	0.146
4	Two-region	Center	31.5	1.392	1.532	1.20	1.078	33.5	40.4	0.108	0.124
5a	Two-region	Diagonal	18.25	1.392	1.532	1.38	1.078	22.50	38.1	0.072	0.083
5b	Two-region	Diagonal	31.0	1.392	1.532	1.38	1.078	33.5	54.8	0.104	0.120

* Applied to inner tubes at first equivalent radius.

D. Application of Hot Channel and Flux Peaking Factors

The three hot channel factors, $F_{\Delta T}$, F_{θ}, F_{q} are applied to that side of the subassembly closest to the center of the core in order to achieve a maximum power (or heat) output on one side of the assembly. By an inspection of Figure 2, it can be seen that the power density or heat output decreases with increasing radius, and therefore the innermost radius on a subassembly has the greater heat output. It is at this radius that hot channel factors are applied. The flux peaking factors F_{fp} are applied only when the subassembly is in the vicinity of a control rod or follower. If a center traverse is taken through a subassembly, a factor of 1.20 is applied and if a diagonal traverse is taken the factor becomes 1.38.

1. Flux Distribution in a Unit Cell

A computer analysis will yield the thermal neutron flux distribution in a unit fuel assembly contained between two moveable control rods for the following conditions:

a. Both control rods are in the core and the flux approaches zero at the boundary of the unit cell.

b. A control rod is in and a follower is out. The flux gradient is of the same sign throughout the traverse and represents the worst flux conditions since thermal deflection of all subassemblies occurs in one direction.

c. Both control rods are out and the followers are in the core. The flux has a finite value at the boundary.

Figure 7 shows the flux distribution versus distance for the above conditions for a diagonal traverse in a unit cell for the Yankee definitive first core for uniform loading of 3.00% enrichment. Similarly, Figure 8 shows the flux distribution for a center traverse.

E. Maximum Temperature Difference

The maximum mean clad temperature difference will occur over the cross-section of a subassembly in that location which will give the most pessimistic combination of hot channel and flux peaking factors. A sample calculation is given in Appendix A which illustrates the method used. Of the analyses conducted thus far, it appears that a temperature difference of 47.4°F will occur in the uniformly enriched Yankee definitive first core which produces a total maximum bowing of 0.146 inches. The maximum bowing in the two region core is 0.124 inches which is substantially less than that in the uniform core.

F. Thermal Deflection Computation - Linear Case

The bowing computations for the linear case are based upon a linear clad temperature difference across the cross-section. Consider the beam of unit width shown below, to have a linear temperature gradient imposed upon it.

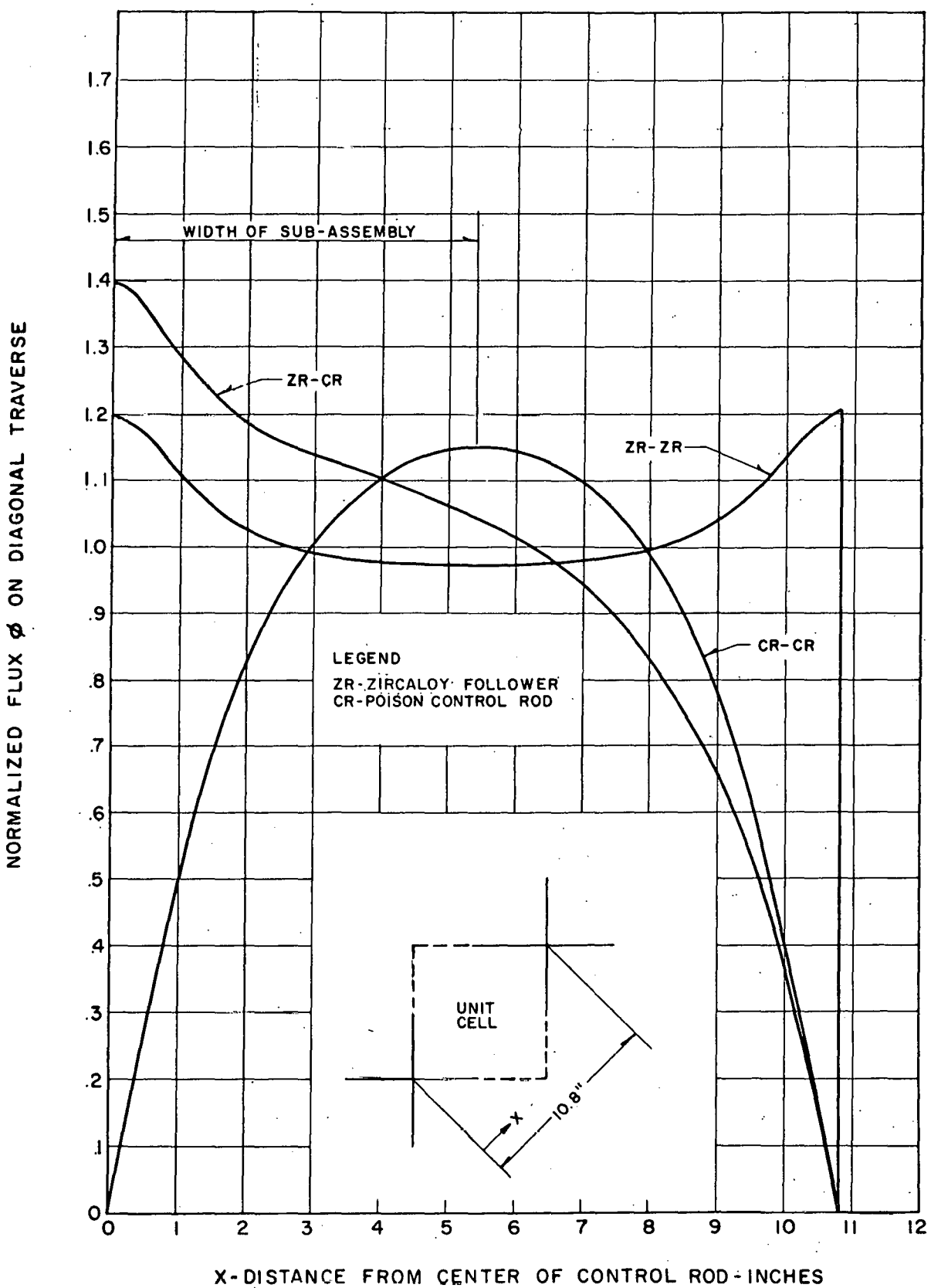

FIGURE 7 FLUX VERSUS DISTANCE FOR A DIAGONAL TRAVERSE IN A UNIT CELL FOR TYPICAL REACTOR WITH CORE FOR UNIFORM ENRICHMENT OF 3.00%.

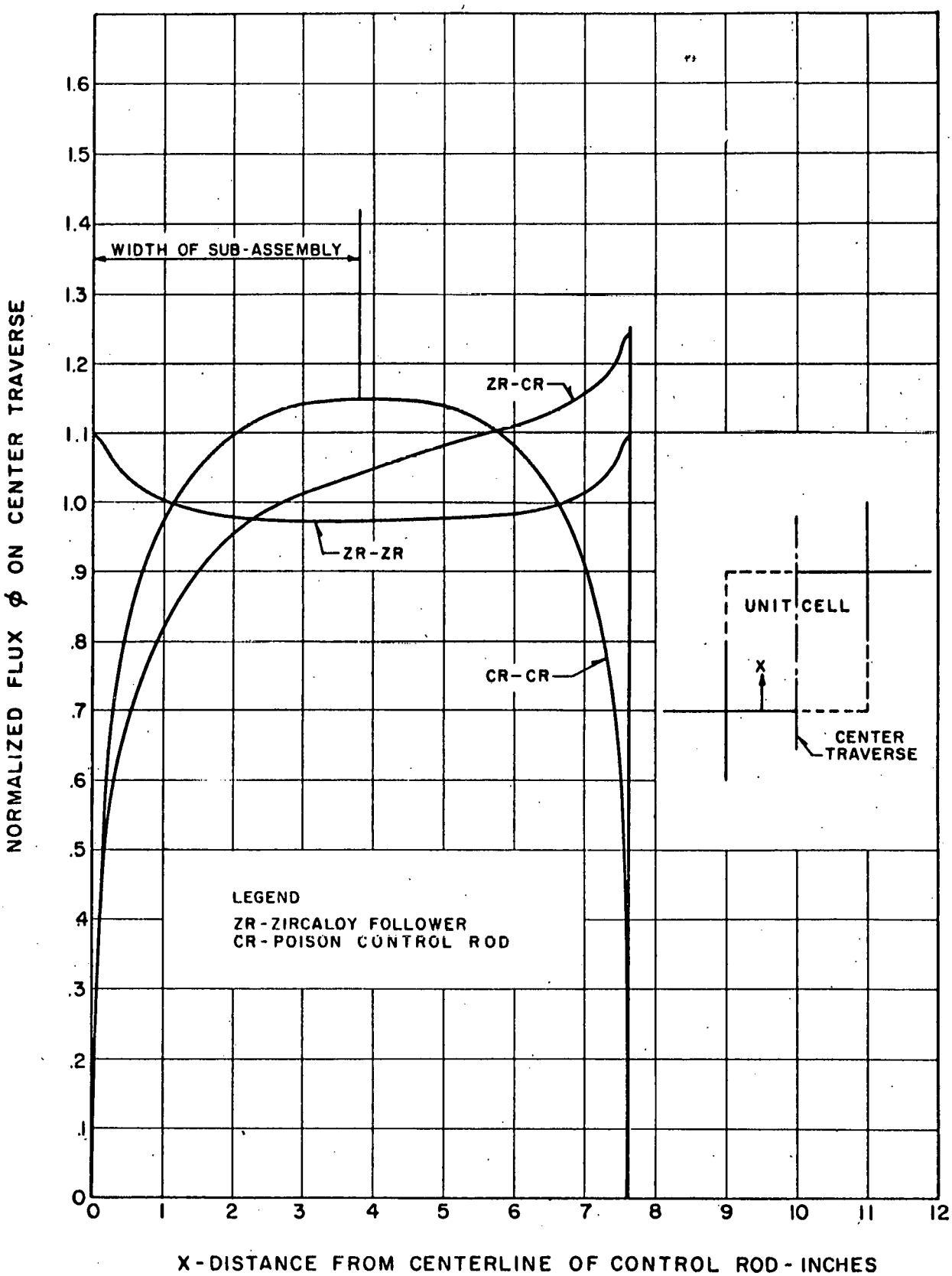

Fig. 8 - FLUX VERSUS DISTANCE FOR CENTER TRAVERSE IN A UNIT CELL FOR TYPICAL REACTOR WITH CORE FOR UNIFORM ENRICHMENT OF 3.00%.

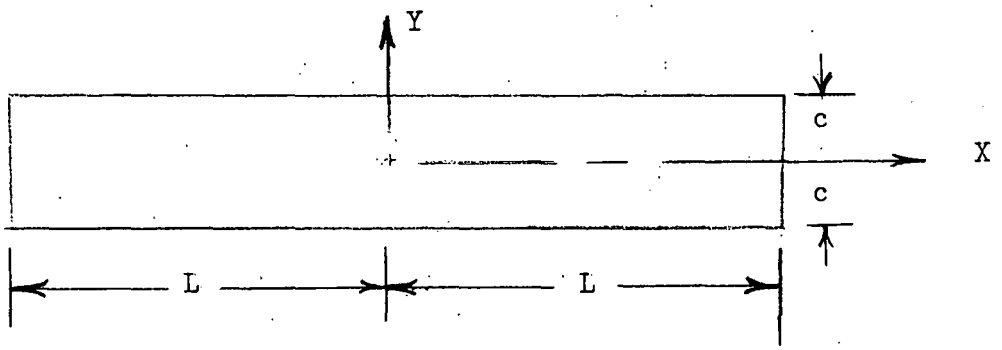

Figure 9 (a)

Unit Beam

The beam will bow in a perfect arc since

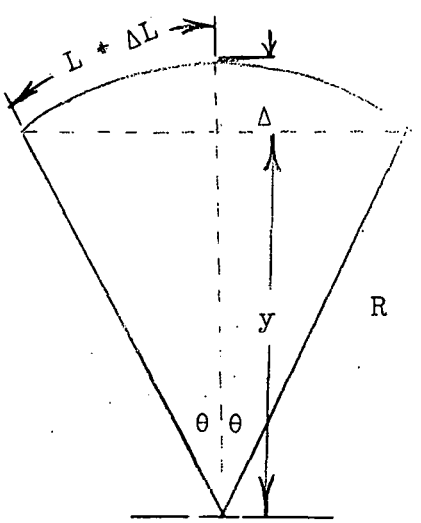

$$\varepsilon_x = \frac{c}{R}$$

$$\text{and} \quad \varepsilon_x = \alpha \frac{\Delta T_c}{2} \qquad (13)$$

$$\therefore \quad R = \frac{C}{\varepsilon_x} = \frac{c}{\alpha \cdot \frac{\Delta T_c}{2}} = \frac{2c}{\alpha \cdot \Delta T_c}$$

Figure 9

Bowing of a Unit Beam

1. Geometrical Derivation

The deflection Δ, can be computed from the following geometrical derivation:

$$y = R \cos \theta$$
$$R = y + \Delta$$
$$\Delta = R - y = R - R \cos \theta = R (1 - \cos \theta)$$
$$L + \Delta L = R\theta \quad \text{but } \Delta L \approx 0$$
$$\therefore \theta = \frac{L}{R}$$

By series expansion

$$\cos x = 1 - \frac{x^2}{2!} + \frac{x^4}{4!} - \frac{x^6}{6!} + \cdots$$

and taking only the first two terms

$$\Delta = R\left[1 - \left(1 - \frac{L^2}{2R^2}\right)\right] = \frac{L^2}{2R} = \frac{L^2}{2\left(\frac{2c}{\alpha \cdot \Delta T_c}\right)}$$

Therefore the deflection becomes

$$\Delta = \frac{\alpha \cdot L^2 \cdot \Delta T_c}{4c} \qquad (14)$$

2. Theoretical Derivation from Theory of Beams

Assume that the linear temperature distribution can be represented by the function, Figure X,

$$T = T_o y \qquad \text{where } C = 1$$

The equation for σ_x [1]* is written so that y = o is at the center axis of the beam.

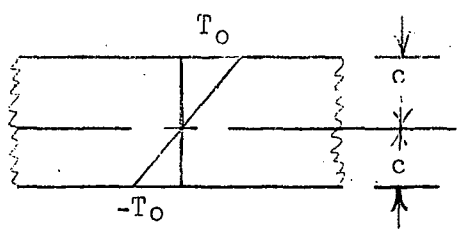

$$\sigma_x = \alpha ET + \frac{1}{2c}\int_{-c}^{+c} \alpha ET\,dy + \frac{3y}{2c^3}\int_{-c}^{+c} \alpha ET \cdot y \cdot dy$$

Figure 10

Linear Temperature Gradient on Unit Beam

---

* Superscripts in parentheses refer to References

substituting $T = T_o y$, the expression for σ_x becomes

$$\sigma_x = \alpha E T_o y + \frac{1}{2} \int_{-1}^{+1} \alpha E T_o y dy + \frac{3y}{2} \int_{-1}^{+1} \alpha E T_o y^2 dy$$

$$\frac{\sigma_x}{\alpha E T_o} = y + \frac{1}{2}\left[\frac{y^2}{2} \right]_{-1}^{+1} + \frac{3y}{2}\left[\frac{y^3}{3} \right]_{-1}^{+1} = 0$$

$$\therefore \quad \sigma_x = 0 \qquad \sigma_z = 0$$

$$\sigma_y = 0 \qquad T_{xy} = 0$$

The strains become

$$\varepsilon_x - \alpha T = \frac{1}{E}(\sigma_x - \nu \sigma_y) = 0$$

$$\varepsilon_y - \alpha T = \frac{1}{E}(\sigma_y - \nu \sigma_x) = 0$$

$$\therefore \quad \varepsilon_x = \frac{\partial u}{\partial x} = \alpha T = \alpha T_o y$$

$$u = \alpha T_o xy + f(y)$$

$$\varepsilon_y = \frac{\partial v}{\partial y} = \alpha T = \alpha T_o y$$

$$v = \frac{\alpha T_o y^2}{2} + f(x)$$

$$\gamma_{xy} = \frac{\partial u}{\partial y} + \frac{\partial v}{\partial x} = 0 = \alpha T_o x + \frac{\partial f(y)}{\partial y} + \frac{\partial f(x)}{\partial x}$$

$$\therefore \frac{\partial f(y)}{\partial y} = 0, \quad f(y) = C_1$$

$$\frac{\partial f(x)}{\partial x} = -\alpha T_o x, \quad f(x) = -\frac{\alpha T_o x^2}{2} + C_2$$

$$\therefore u = \alpha T_o xg + C_1$$

$$v = \frac{\alpha T_o y^2}{2} - \frac{\alpha T_o x^2}{2} + C_2$$

The displacements u and v are determined by evaluating the boundary conditions given below:

at $x = 0, y = 0$ let $u = 0$ at $x = \pm L, y = 0$ let $v = 0$

$\therefore C_1 = 0$ $C_2 = \frac{\alpha T_o L^2}{2}$

Therefore the displacements become

$$u = \alpha T_o xy$$

$$v = \frac{\alpha T_o}{2} (y^2 - x^2 + L^2)$$

and at $y = 0$

$$v = \frac{\alpha T_o}{2} (L^2 - x^2)$$

When $x = 0, v = \Delta_{max}$

$$\Delta_{max} = \frac{\alpha T_o L^2}{2} \qquad (15)$$

This result, equation (15) is the same as obtained above in equation (14) for the geometrical derivation, when the linear temperature distribution is expressed in equation form as $T = T_o y$.

3. The Case of Local Temperature Differences Along Axis

Instead of assuming a constant temperature difference across the subassembly along the axis, the local variations in temperature difference can be taken into account by a numerical step by step analysis in which the arcs generated by the temperature difference are added together. The thermal deflection computed from this analysis, shown in Figure 11, revealed that the total deflection or bowing due to local conditions is about 15% greater than that due to average conditions. Consequently, in actual practice, the average thermal deflection should be multiplied by a factor of 1.15 to account for local variations. However, this feature is not explored in the remaining portion of this work, since it would constitute a separate investigation in itself.

G. Thermal Deflection Computation - Non-Linear Case

Since the most general case of thermal deflection involves deflections from non-linear temperature distributions, there should be some general method which will accurately predict deflection under any arbitrary temperature distribution. The

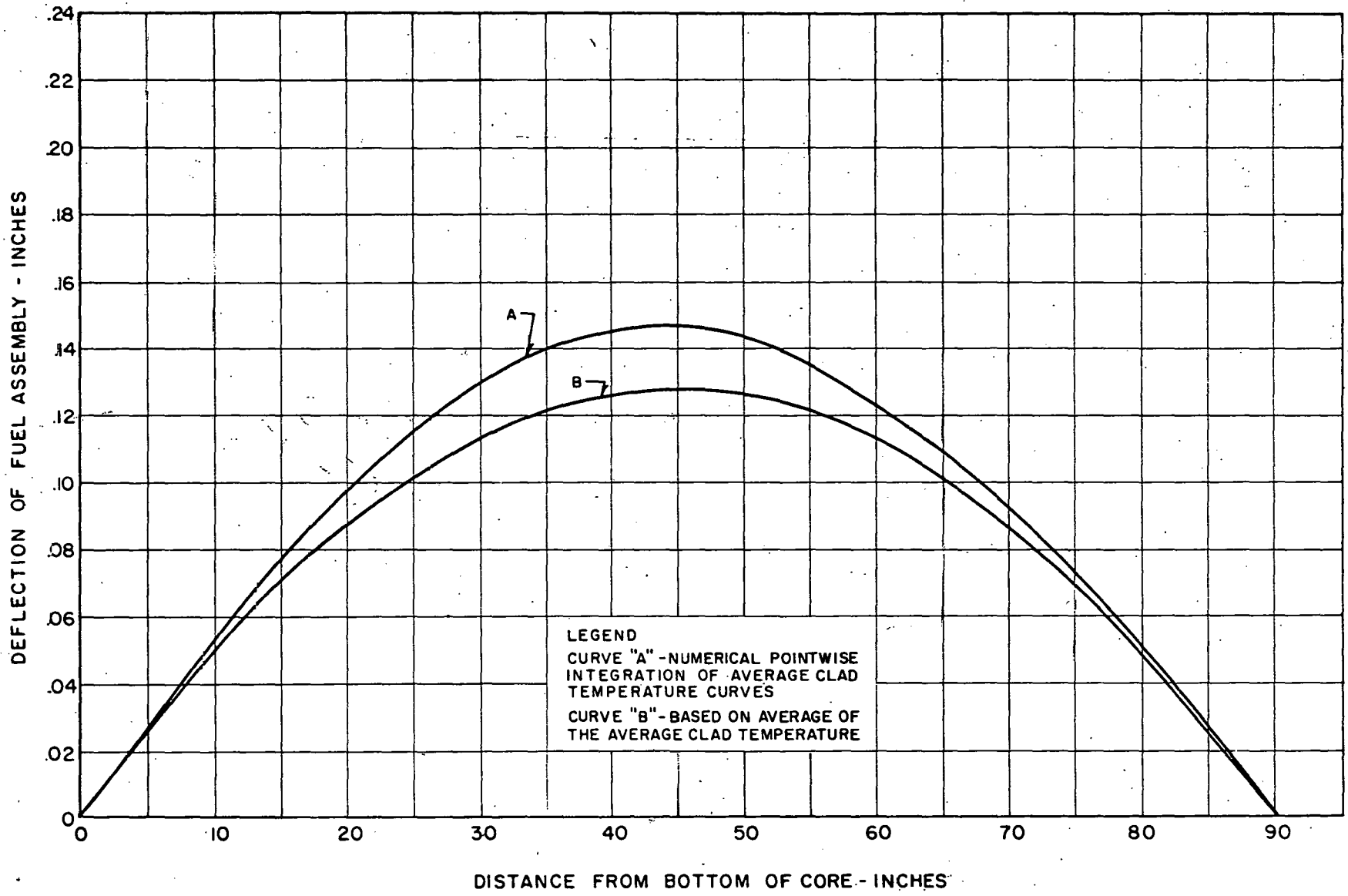

FIGURE 11 DEFLECTION VERSUS LENGTH FOR REACTOR FUEL SUB-ASSEMBLY WITH A LINEAR ONE-DIMENSIONAL THERMAL GRADIENT BASED ON AVERAGE CLAD TEMPERATURE ACROSS THE CROSS-SECTION.

general case, therefore, necessarily includes the linear case, so that the results computed in the previous section can be considered as a special case. In the first attempt at deriving the general case, the subassembly was considered to be a unit beam of solid cross-section. By considering the temperature to be a function of one - variable alone, e.g. a function of y only, the thermal stress equation is developed which yields the thermal stress as a function of the distance y. From the thermal stress equation, the thermal strains are found by Hooke's Law. The respective displacements corresponding to the strains can be found by applying boundary conditions which depend upon the method of loading and support. The displacement v in the vertical direction will yield the deflection Δ at the center of the beam under appropriate conditions. As will be demonstrated under Section V, this method of solution is not accurate as the temperature distribution becomes more and more non-linear, but the analysis is included because it is fundamental to the understanding of the correct method of solution, namely, the numerical summation method.

1. Thermal Stress Equation

When a beam is subjected to a non-linear temperature distribution, expansion within a continous body cannot proceed freely and stresses due to non-uniform heating are set up. Consider a thin rectangular beam of unit thickness throughout its length in which the temperature T is a function of y (Figure 12) and is independent of x and z.

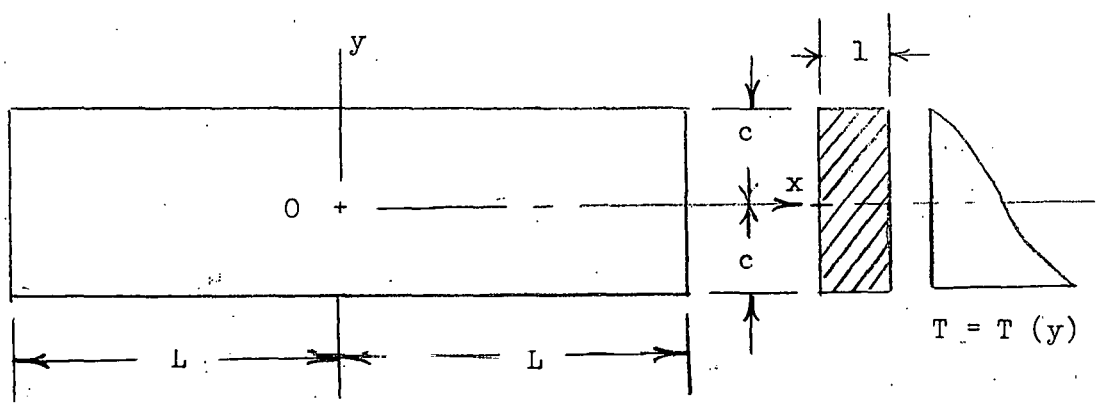

Figure 12

Non-Linear Temperature Gradient on Unit Beam

Timoshenko[2] and Goodier have developed a thermal stress function x for a unit width solid rectangular beam which has a non-linear temperature distribution imposed upon the beam as a function of one variable y.

The total stress for this beam is

$$\sigma_x = -\Sigma \alpha . E . T(y) + \frac{1}{2c}\int_{-c}^{+c} \alpha E . T(y) \cdot dy + \frac{3y}{2c^3}\int_{-c}^{+c} \alpha E . T(y) . y dy \qquad (16)$$

where T (y) is the temperature function. The above equation (16) is the resultant thermal stress in the beam which is composed of the sum of compressive stress, the induced tensile stress and the bending stress for unequal expansion.

A. Derivation of Center Deflection - Solid Beam Method

The general equations for thermal strains from Hooke's Law are:

$$\begin{aligned} \varepsilon_x - \alpha \cdot T(y) &= \frac{1}{E} \sigma_x - \nu (\sigma_y + \sigma_z) \\ \varepsilon_y = \alpha \cdot T(y) &= \frac{1}{E} \sigma_y - \nu (\sigma_x + \sigma_x) \\ \varepsilon_z = \alpha \cdot T(y) &= \frac{1}{E} \sigma_z - \nu (\sigma_x + \sigma_y) \end{aligned} \tag{17}$$

which reduce to the following form since $\sigma_x = f(y)$ and $\sigma_y = \sigma_x = 0$

$$\begin{aligned} \varepsilon_x - \alpha \cdot T(y) &= \frac{1}{E} \sigma_x \\ \varepsilon_y - \alpha \cdot T(y) &= - \frac{1}{E} \sigma_x \\ \varepsilon_z - \alpha \cdot T(y) &= - \frac{1}{E} \sigma_x \end{aligned} \tag{18}$$

Since the beam is of unit thickness the z direction, ε_z can be eliminated from the analysis. The above equations rewritten become

$$\begin{aligned} \varepsilon_x &= \frac{\partial u}{\partial x} = \alpha \cdot T(y) + \frac{1}{E} \sigma_x \\ \varepsilon_y &= \frac{\partial v}{\partial y} = \alpha \cdot T(y) - \frac{\nu}{E} \sigma_x \end{aligned} \tag{19}$$

The displacements u, and v are found by integrating the above equations and by solving for the constants of integration from boundary conditions. The complete derivation is found in Reference 9. The displacement v equals the deflection Δ when y = 0.

When x = 0, at the center of the beam, $\Delta = \Delta_{max}$ so that the maximum deflection becomes

$$\Delta_{max} = \frac{\alpha L^2}{2} \frac{\partial T(y)}{\partial y} + \frac{L^2}{2E} \frac{\partial \sigma_x}{\partial y} \tag{36}$$

A numerical example of this procedure is presented in Appendix B for the temperature function $T = 50\ e^{-4y} - 4.4$. The discussion of the results of such a method are presented in Section V.

2. Numerical Summation Method

In the analysis contained in Section 1 above, the beam was assumed to behave as a solid rectangular beam of unit width with isotropic characteristics in three directions. There is no justification for such an assumption. The beam is not solid and does not have isotropic characteristics. Therefore, the stress function, equation (16), derived for the solid beam must be modified so as to apply to a unit tubular beam. Equation (16) is written below for reference only

$$\sigma_x = -\alpha E \cdot T(y) + \frac{1}{2c}\int_{-c}^{+c} \alpha E \cdot T(y)dy + \frac{y}{\frac{2}{3}c^3}\int_{-c}^{+c} \alpha E \cdot T(y) \cdot y dy \qquad (37)$$

The first term of the above equation depends upon the temperature function $T(y)$ only, and is independent of the properties of the beam. The second and third terms, however, depend upon the specific properties of Area A, and moment of intertia I, respectively, of the beam. In the second term, the coefficient, $\frac{1}{2c \cdot 1}$ which represents the inverse of the unit area of solid beam, should be replaced by the actual total area A of the tubular beam, namely, $\frac{1}{A}$. The integral part of the second term represents a tensile force exerted on the beam at a considerable distance from the ends and is an exact integral for the temperature function. However, the beam consisting of 36 tubes of 6 tubes per row constitutes a step-wise temperature function of which the exact integral is somewhat of an approximation. The integral should be therefore replaced by a summation function Σ, where αE are constants, $T(y)$ is now represented by the temperature T in the tube at that location and 1 times dy, i.e. the area, is replaced by the exact area of one row of tubes. The Σ function is summed over the six rows to include the whole beam. It will be noted from the calculation in Appendix B, however, that the deflection Δ, is not dependent at all upon the value of the second term, but rather on the coefficient of y in the third term. In a similar manner, the moment of inertia, i.e. $\frac{2}{3}c^3$ of the solid beam in the third term, is replaced by the actual moment of interia I of the whole beam. The integral is also replaced by the more exact Σ term and as before, the temperature function $T(y)$ is replaced by the actual temperature T at that point, and 1 times dy, i.e. the area, is replaced by the actual area of one row of tubes. In addition, y is replaced in each case, by the centerline distance from the center of the tube bundle cross-section to the centerline of each tube row. The summation is then performed over the fuel tube cross section. When all of these substitutions are made, the modified and correct solution for the thermal stress becomes

$$\sigma_x = -\alpha E \cdot T(y) + \frac{1}{A}\sum_{1}^{N} \alpha E \cdot T_N \cdot A_N + \frac{y}{I}\sum_{1}^{N} \alpha E \cdot T_N \cdot y_N \cdot A_N \qquad (38)$$

where the N function refers to tube row under analysis. In every case, where the temperature function is represented by a single variable, y, the thermal stress function reduces to the form

$$\sigma_x = a \circ T(y) + b - cy \qquad (39)$$

for a particular temperature function, where a, b and c are constant coefficients. The same analysis is now performed on the stress function as described in Section III, G, 1, a, to obtain the strains, the displacements and eventually the deflection of the fuel bundle. The results show that the maximum deflection is dependent only upon the coefficient c, in the third term of equation (39), and that the deflection can be represented in general by the equation

$$\Delta_{max} = - \frac{CL^2}{2E} \qquad (40)$$

A numerical calculation of the numerical summation method is presented in Appendix C for the temperature function $T = 50e^{-4y-4A}$. The results can be compared to the calculation in Appendix B, which yields the deflection by the first method. Comparison will be made in Section V of all temperature functions investigated.

H. Consideration of Mechanical Tolerance Buildup

In addition to the thermal deflection occurring in a fuel assembly reducing the clearance between a control rod and fuel assembly, mechanical tolerances may be such as to further reduce the available clearance. Table II shows the mechanical tolerance build-up in the Yankee reactor from actual design tolerances and estimates. The mechanical tolerance build-up is sufficient to be of concern and is as important to clearance considerations as is the accurate determination of thermal deflection.

A summary of the clearance available in the Definitive Design and Compromise Design Fuel Assemblies is given in Table III which includes fuel assembly design data and thermal bowing results. From this table it can be seen that the definitive design could produce an interference of 0.077 inch, whereas the compromise design is designed so as to have a net clearance of 0.001 inch in the worst possible case.

TABLE II

MECHANICAL TOLERANCE BUILD-UP IN YANKEE REACTOR FOR REDUCTION OF CLEARANCE BETWEEN CONTROL ROD AND DEFINITIVE DESIGN FUEL ASSEMBLY

1.	Misalignment of Fuel Assembly Bundles with Centerline of End Nozzles	0.020 "
2.	Bowing or Permissible Distortion in Fuel Tubes Throughout Their Length	0.060
3.	Clearance on Diameter of End Nozzle and Hole in Support Plate	0.008
4.	Additional Tolerance	0.009
5.	Bowing Tolerance on Control Rod	0.015
	Sum	0.115
	Nominal Clearance Between Control Rod and Fuel Assembly Plus Guide Clearance	0.181
	Minus Sum of Mechanical Tolerance Build-up	-0.115
	Clearance Available for Deflection	0.069"

TABLE III

FUEL ASSEMBLY DESIGN DATA AND THERMAL BOWING RESULTS

Design Parameters	Definitive Design	Compromise Design
Subassembly Size	9 x 9	6 x 6
Fuel Rod Pitch	0.425"	0.422"
Control Rod Thickness	0.285	0.265
Nominal Clearance	0.119	0.123
Guide Clearance	0.062	0.095
Fabrication Bowing	0.060	0.060
Socket Tolerance	0.020	0.020
Control Rod Bowing	0.015	0.015
Additional Tolerance	0.019	0.017
Thermal Bowing	0.146	0.105
Net Clearance	-0.077"	+0.001"

VII. EXPERIMENTAL TESTING OF FUEL SUB-ASSEMBLY

In order to check the method of theoretical calculation, an experimental program was conducted on a 6 x 6 array, tubular fuel assembly. The fuel subassembly was composed of hollow fuel tubes and ferrules (or spacers between tubes) with the following dimensions:

(a) fuel tube outside diameter = 0.337"
(b) fuel tube inside diameter = 0.295"
(c) pitch of fuel tubes (y and z directions) = 0.441"
(d) ferrule outside diameter = 0.287"
(e) ferrule inside diameter = 0.257"
(f) ferrule length = 0.500"
(g) pitch of ferrules (x direction) = 12.0"
(h) length of fuel subassembly = 95.0"

Views of the experimental setup are shown in Figure 13 and 14, illustrating the fuel subassembly with water connections, thermocouples, potentiometer, dial gages, cathetometer and other apparatus. Any desired linear or non-linear temperature gradient could be obtained with this apparatus.

Seven different temperature functions were imposed upon the fuel assembly. The basic equations are listed below and were arbitrarily chosen to give linear and non-linear temperature gradients, with an approximate overall temperature difference of 50°F. The temperature functions are:

(a) $T = \frac{50}{2.2} \sqrt{4.84 - y^2}$

(b) $T = 50 \cos \frac{\pi}{4.4} y$

(c) $T = 50 - 22.7\ y$ (this is the linear gradient)

(d) $T = 50\ e^{-y}$

(e) $T = 50\ (.25)^y$

(f) $T = 50\ e^{-2y}$

(g) $T = 50\ e^{-4y}$

The temperatures corresponding to the pitch distances of 0.440" and multiples thereof, were calculated and imposed upon the tubular beam. Table IV shows the experimental results for each temperature function across the fuel subassembly. The temperature difference, i.e. the temperature above a datum of 60°F, is shown as a function of y.

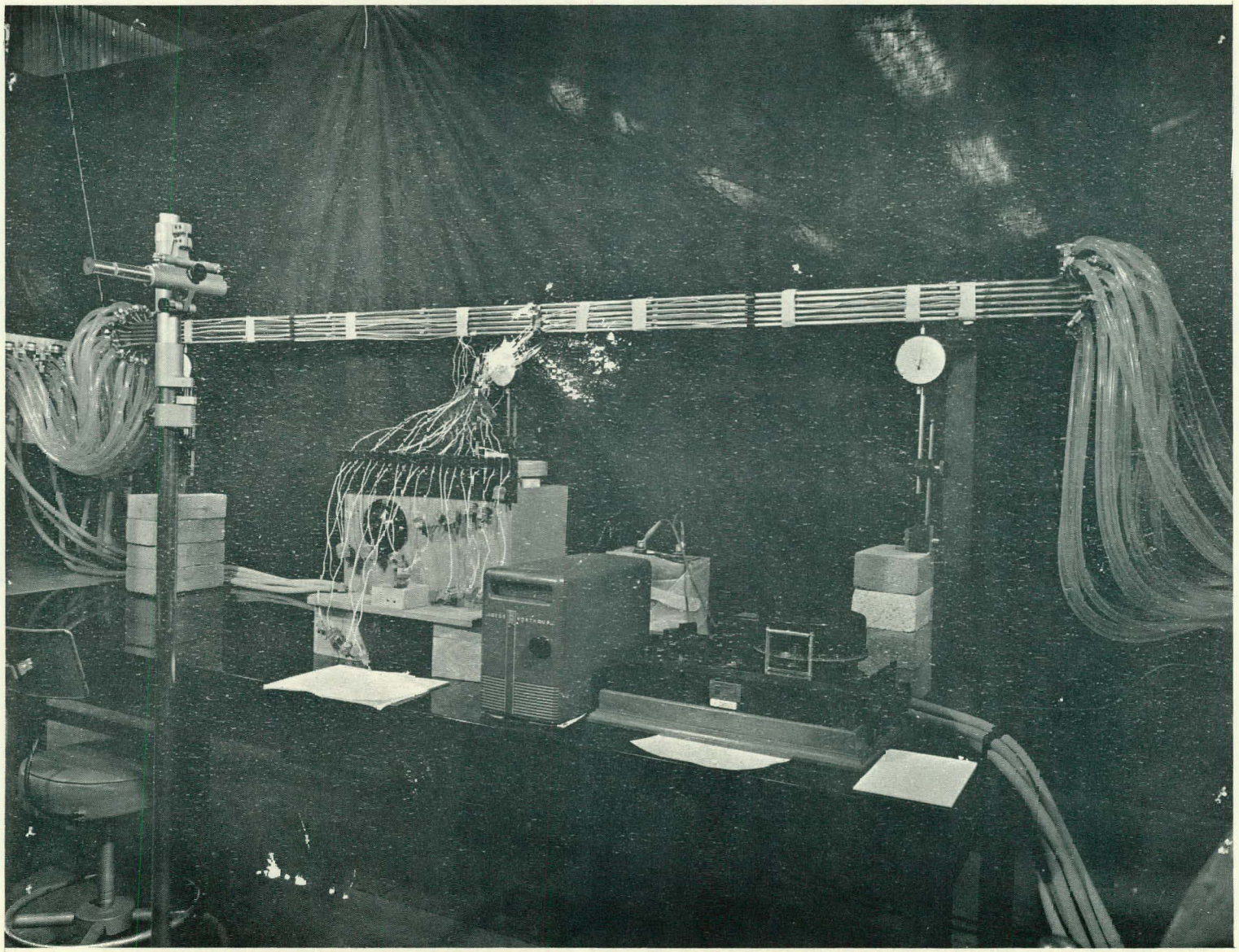

FIGURE 13 RIGHT HAND VIEW OF FUEL SUBASSEMBLY THERMAL DEFLECTION TEST EQUIPMENT

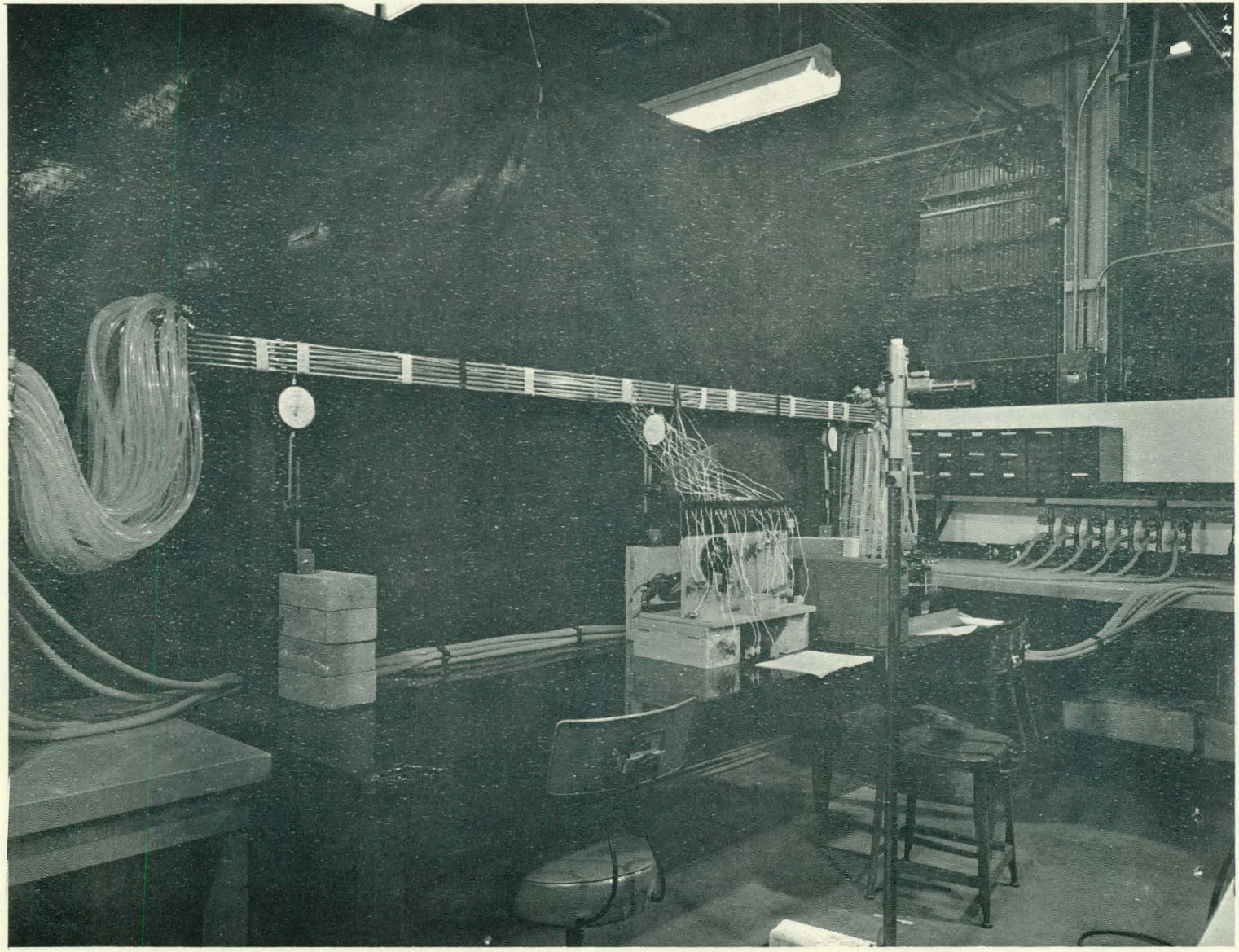

FIGURE 14 LEFT HAND VIEW OF FUEL SUBASSEMBLY THERMAL DEFLECTION TEST EQUIPMENT

TABLE IV

TABLE OF EXPERIMENTAL RESULTS FROM LINEAR AND NON-LINEAR TEMPERATURE GRADIENTS ACROSS REACTOR SUB-ASSEMBLY.

TEMPERATURE FUNCTION	TEST NO.	TEMPERATURE DIFFERENCE	DISTANCE y						TEST Δ	AVG Δ_{TEST}	EXTRAPOLATED* Δ_E
			0	0.44	0.88	1.32	1.76	2.2			
$T = \frac{50}{2.2}\sqrt{4.84 - y^2}$	1		49.5	48.5	47	38.5	31	0	0.146	0.150	0.150
	2		50	47.5	45.7	39	28.5	0	0.1535		
$T = 50 \cos \frac{\pi}{4.4} y$	1		50	47.5	40	29.4	15	0	0.169	0.170	0.170
	2		50	47.5	40.3	29	15	0	0.171		
$T = 50 - 22.7 y$	1		50	37.5	29	21	12	0	0.171	0.171	0.171
	2		50	39	31	22	9	0	0.171		
$T = 50 e^{-y}$	1		51.5	33.2	22	18	11.5	5.5	0.148	0.148	0.166
	2		48	33.5	21.5	9.5	7.5	5.5	0.148		
$T = 50 (.25)^y$	1		50	29.3	14.7	8	4.3	2.3	0.157	0.156	0.163
	2		50	27.6	13.8	8	4.3	2.3	0.155		
$T = 50 e^{-2y}$	1		50	22	7.5	2	0	0	0.155	0.154	0.154
	2		50	21.5	8.6	3.5	2	0	0.153		
$T = 50 e^{-4y}$	1		50	7	.5	1.5	0	0	0.126	0.125	0.125
	2		50	8.6	2	0	0	0	0.124		

* The Extrapolation Deflection Δ_E, is the expected deflection if a 50°F gradient occurred in each temperature profile. It is included for comparison purposes.

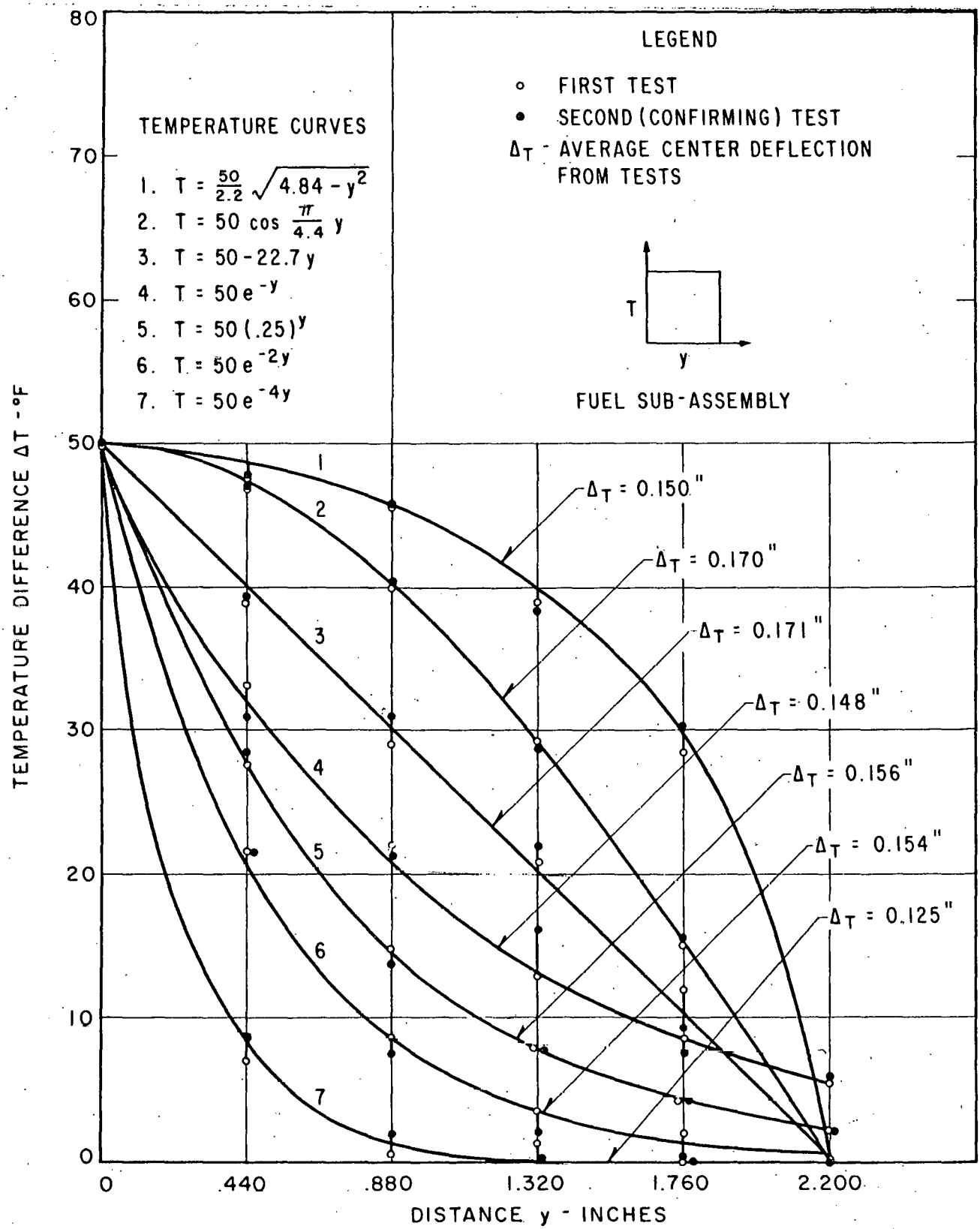

FIGURE 15

EXPERIMENTAL RESULTS OF CENTER DEFLECTION OF SUBASSEMBLY FROM LINEAR AND NON-LINEAR TEMPERATURE GRADIENTS ACROSS SUBASSEMBLY

Two or more tests were run for each temperature distribution until confirming results were achieved. The deflection was measured accurately in each case and recorded. The average deflection from test, Δ_{test}, was computed from the two deflection readings. An extrapolated deflection, Δ_E, is the expected deflection if a 50°F gradient occurred in each temperature profile. It is included for comparison purposes. An additional linear test of 30°F was imposed on the fuel assembly and was found to be exactly proportional to the deflection from a 50°F gradient. A plot of the experimental data is shown in Figure 15 with the theoretical curves superimposed on the experimental results to show the accuracy of each point. The experimental points, however, represent a step function in temperature, since the row of tubes at each location are all at the same temperature. The test average center deflections are also included on the plot for ready reference. In 95% of the cases, the temperature points do not deviate from the theoretical points by more than ± 1°F.

A. Thermal Experimental Procedure and Results

Each of the tests followed the same experimental procedure. Cold water, at 60°F was run through all of the tubes and zero readings were taken on the dial gages and cathetometer. Figure 16 shows the hot and cold water valves that were used to adjust the temperature in each tube row. The temperatures were adjusted to the proper values for the six rows of tubes. The deflection was read on the dial gages and cathetometer and the zero reading was subtracted to obtain the net deflection. Dial gage measurements were taken to the nearest 1/10 of a mil (0.0001 inch). The cathetometer could be read by means of a vernier to 0.05 millimeter (or 0.002 inch). The temperatures for each tube row were taken at four places, two at the inlet and two at the outlet. Because of the mass flow rate of water, there was no noticeable temperature drop over the length of the assembly. Since water occupied the internal volume of the hollow tubes before and after test, the weight of water was subtracted from the net deflection. Deflection measurements were substantiated in all cases and the deflection can be considered accurate to within ± 0.001 inch. All results are indicated in Table IV. Comparison with theoretical calculations will be made in Section V.

B. Mechanical Experimental Procedure and Results

A mechanical end moment test was performed in which a pure bending moment was applied to the tubular beam in order to determine the moment of inertia I, experimentally, for comparison with the theoretical moment of inertia and for use in equation (38) in determining the thermal stress σ_x. In the end moment test, shown in Figure 16, a moment was applied at each end to give a constant moment over the subassembly length between supports. A plot of the experimental results for a number of tests is shown in Figure 17.

In each test, the subassembly deflected in an upward direction and deflections were measured at the center by the cathetometer. Loads of up to 300 pounds in 20 pound increments were applied at the load points specified. Corresponding deflections of the fuel assembly were taken for each load increase. The net deflection is calculated by subtracting the "zero" deflection reading from the deflection reading recorded in each case. The moment of inertia was determined from the actual end moment deflection test as being 0.446 inch to the fourth power. This was determined from the deflection formula for the beam given below as:

$$\Delta = \frac{ML^2}{8EI} \qquad (41)$$

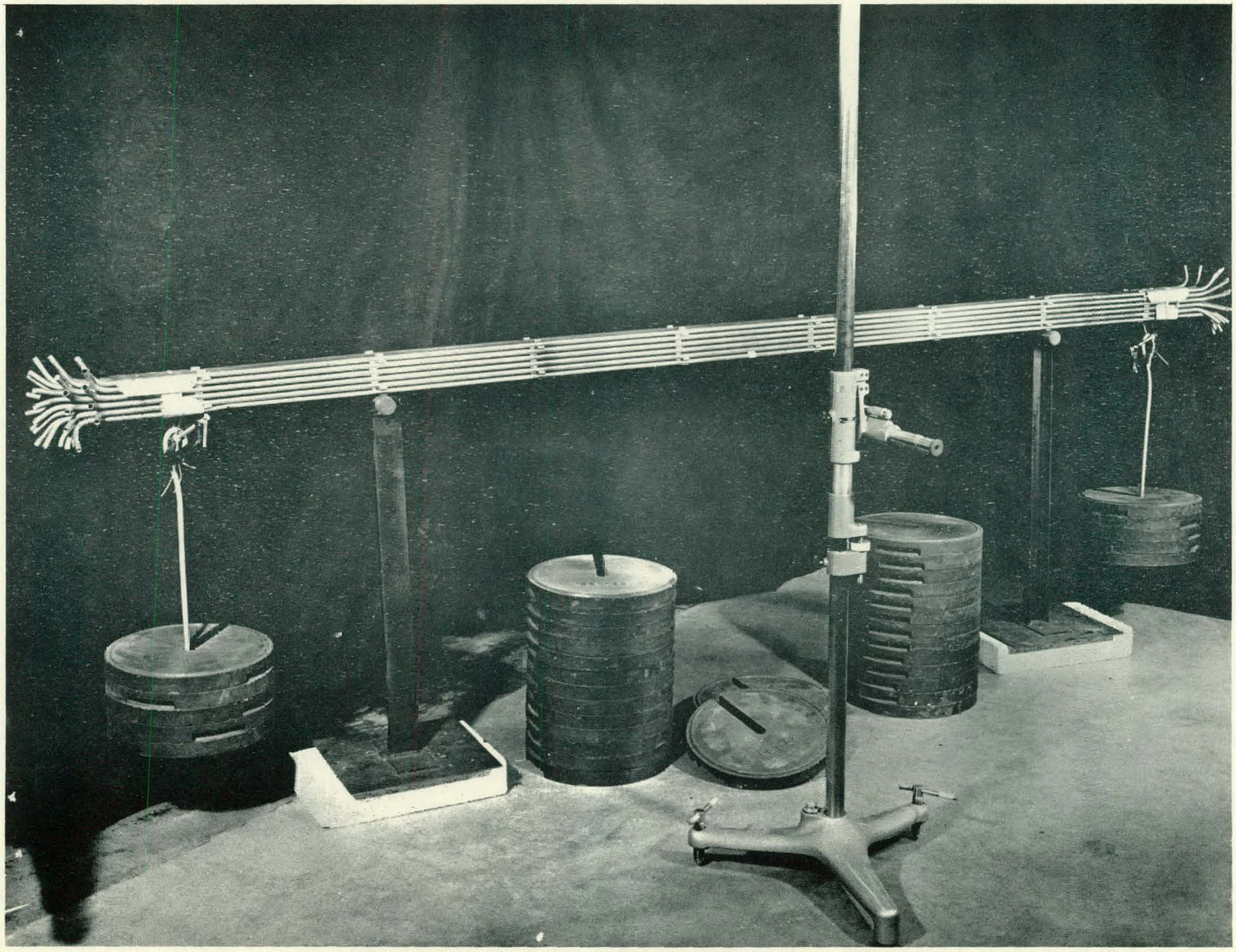

FIGURE 16 END MOMENT DEFLECTION TEST

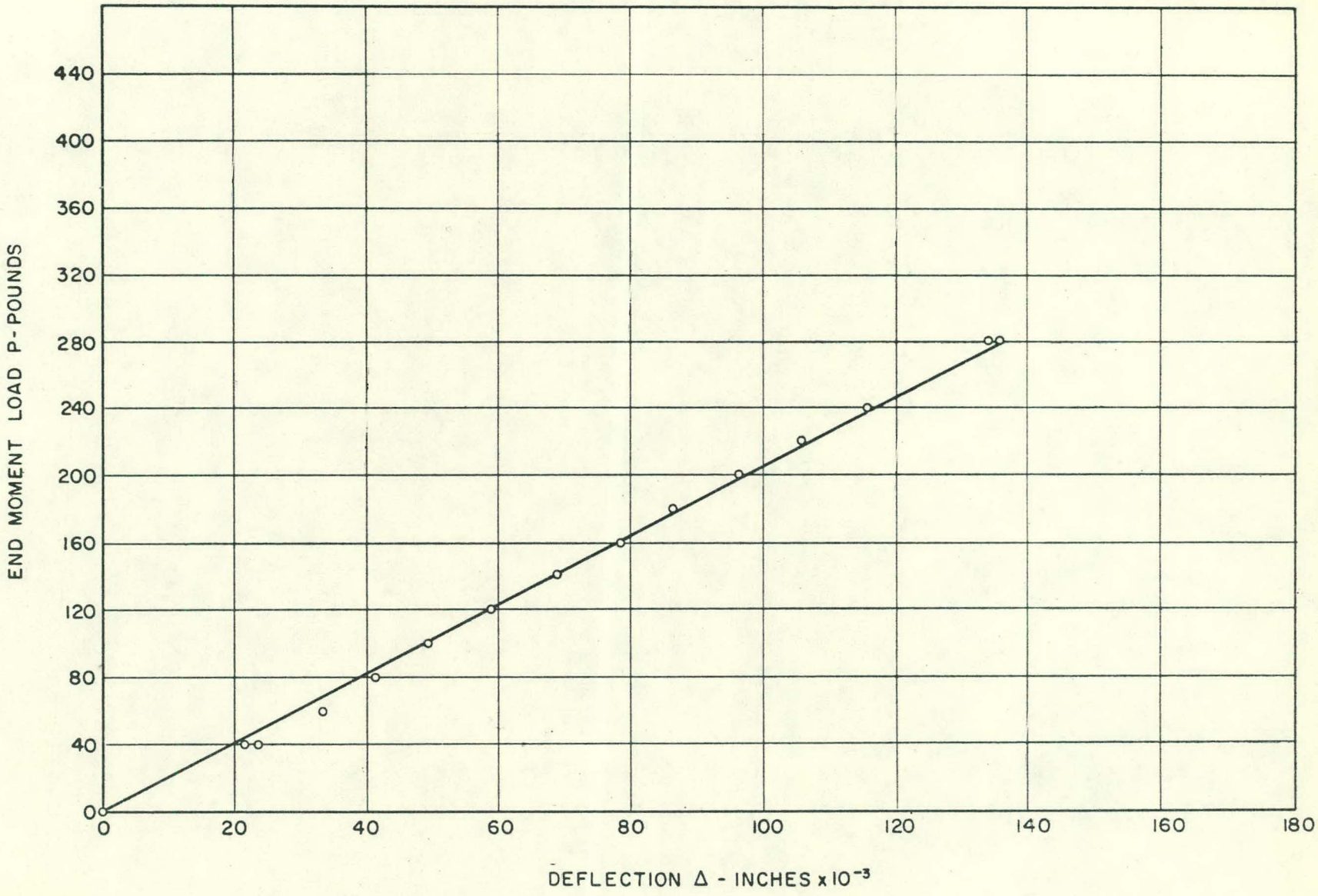

FIGURE 17 END MOMENT LOAD VERSUS DEFLECTION FOR REACTOR FUEL SUB-ASSEMBLY ABOUT TRANSVERSE AXIS. SPAN IS 60 INCHES WITH END MOMENT = 13.5 P FOR 6x6 ARRAY OF 0.337 O.D. AND 0.295 I.D FUEL TUBES WITH PITCH LATTICE OF 0.440 INCHES MOMENT OF INERTIA FROM TEST IS $I = 0.446$ IN.^{4}.

where M is the end moment applied by the end loads and is equal to 13.5 P inch-pounds and L, the length between supports is 60 inches. The theoretical moment of inertia was computed to be 0.4344 inch to the fourth power, which constitutes about a 3% difference from experimental results. This shows excellent agreement between theory and experiment. The experimental value of I = 0.446 inch was used in the calculations shown in Appendix C and in all other numerical summation solutions.

In order to check the shear rigidity of the subassembly a second test was performed on the beam as shown in Figure 18 in which a load was applied at the center and the corresponding deflections were measured by the cathetometer. A plot of experimental results is shown in Figure 19.

In this test, the subassembly deflected downward when loads of up to 120 pounds were applied in 10 pound increments at the center of the beam. The deflections were recorded for each load increase and the net deflection was determined by subtracting the zero reading from the deflection reading recorded in each case.

A theoretical analysis was performed in order to derive a method for predicting the deflection of any subassembly. This analysis attempts to account for shear deformation in a subassembly. The beam is assumed to deflect under the combined effect of bending due to load and shear deformation. The beam is cut in two and treated as a cantilever with a load $\frac{P}{2}$ applied at the end. The deflection due to bending is

$$\Delta_1 = \frac{PL^3}{3EI} \tag{41}$$

and the deflection due to shear is

$$\Delta_2 = \sum_{0}^{N} \frac{PL_N^3}{12\,EI} \tag{42}$$

where L_N is the distance between ferrules. The analysis assumes that each location of ferrules can be considered to be a guided cantilever beam. The Δ_{total} is obtained by adding equations (41) and (42)

$$\Delta_{TOTAL} = \Delta_1 + \Delta_2 = \frac{PL^3}{3EI} + \sum_{0}^{N} \frac{PL_N^3}{12EI} \tag{43}$$

The results of this theoretical analysis showed that the deflection can be predicted to within -7% of experimental deflection. For example, a load of 110 pounds was applied to a subassembly as shown in Figure 18 and a deflection of 0.202 inch was measured. By using a load of 55 pounds (equivalent to P/2) in equation (43) the deflection Δ was computed to be 0.1884 inch, assuming that flexural rigidity IE, was the calculated theoretical value. As the 7% error from theoretical calculations was somewhat greater than expected, an inspection of the fuel subassembly was conducted to determine if manufacturing tolerances had been exceeded. The inspection report indicated that the fuel subassembly was manufactured according to specifications and that design tolerances had not been exceeded.

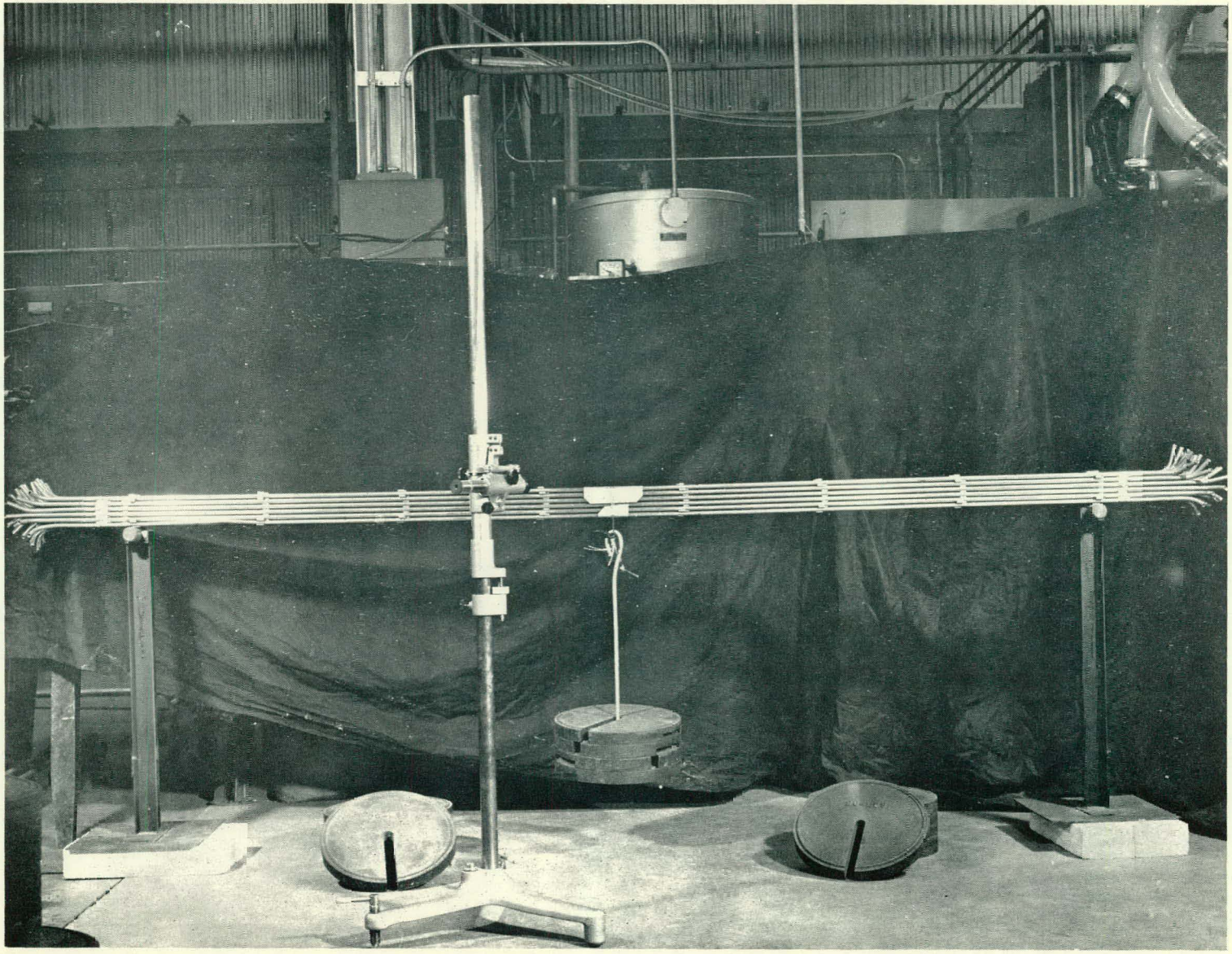

FIGURE 18 CENTER LOAD DEFLECTION TEST

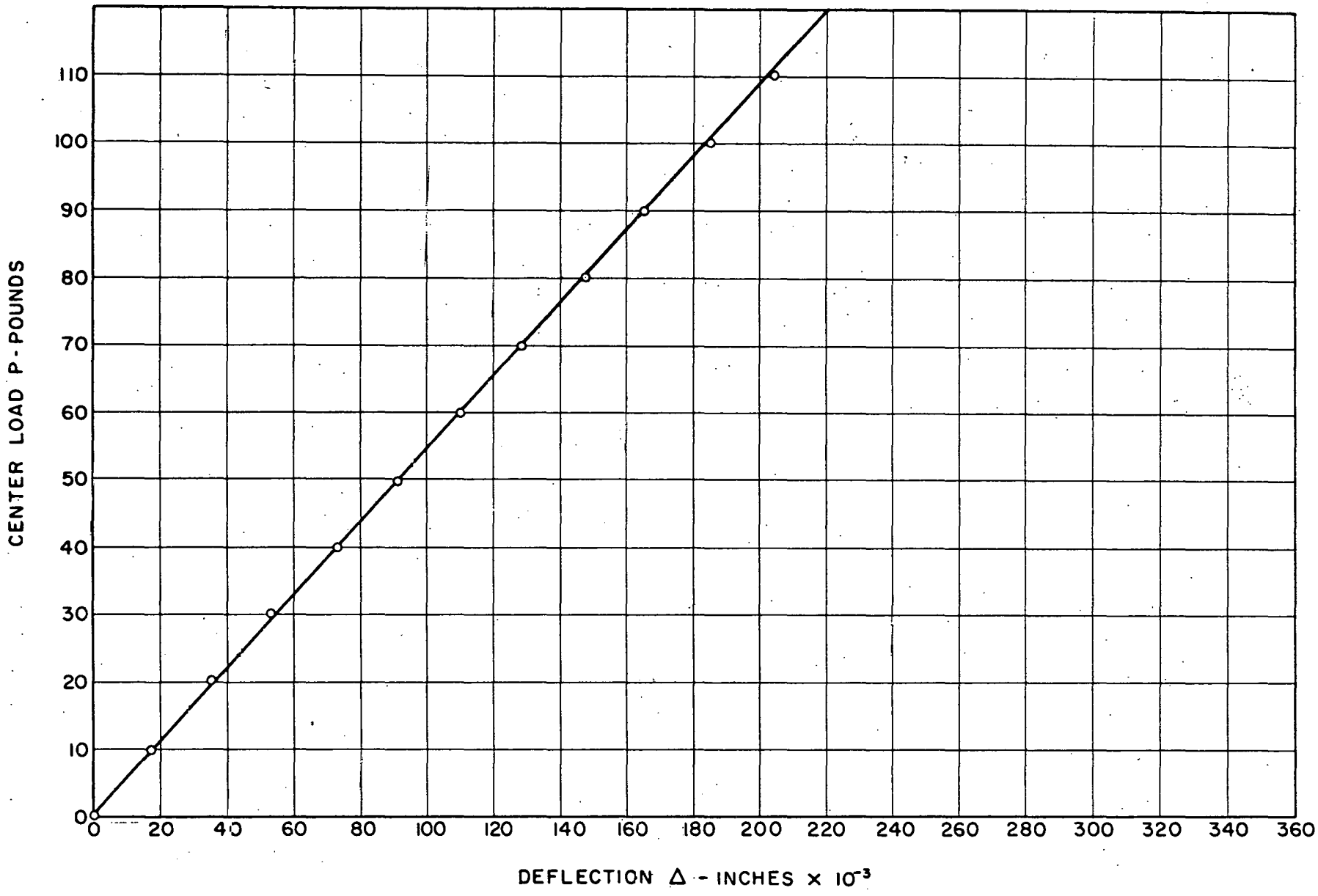

FIGURE 19 CENTER LOAD VERSUS DEFLECTION FOR REACTOR FUEL SUB-ASSEMBLY. SPAN IS $82\frac{3}{4}$" FOR A 6x6 ARRAY OF 0.337 O.D., 0.295 I.D. FUEL TUBES WITH PITCH LATTICE OF 0.441"

The theoretical analysis, therefore, is somewhat in error, but can be used to obtain an approximate solution of center load for a corresponding deflection.

The purpose of conducting the center load deflection test was to determine the load-deflection characteristics of the subassembly so that if interference between a fuel assembly and control rod did occur, the locking force might be computed. It was stated previously that redesign of the definitive design fuel assembly became mandatory to prevent interference with the control rods and that the locking force holding the control rod in a fixed position may be of sufficient magnitude to prevent the control rod from moving within the core. The definitive design fuel assembly may thermally bow to the extent of 0.077 inch interference. The force necessary to bring this deflection back to zero interference is about 150 pounds. Since this force acts in a direction that is perpendicular to the axial center line of the control rod, in addition to equal but opposite reactive forces at the guide blocks in the upper and lower core support plates, the friction force or locking force may be appreciable. The friction force is equal to μN, and assuming μ to be about 1 between stainless steel and Zircaloy in water, and N to be a total of 300 lbs. (150 lbs. at the center, and 75 lbs. at each guide block), the friction locking force may be as high as 300 lbs. which is close to the total weight of the control rod. The friction force is certainly large enough to demonstrate that such a condition cannot be allowed and therefore must be remedied by using the compromise design fuel assembly instead of the definitive design fuel subassembly in the Yankee reactor.

VIII. DISCUSSION OF RESULTS

In deriving the numerical summation method, it was emphasized that there were definite limitations to the application of the solid beam theory to a tubular fuel assembly. Table V contains complete experimental deflection data for each temperature function; the deflections from solid beam theory and the numerical summation method are included for comparison together with the percentage error from the true experimental results. The table shows that in the application of the solid beam theory, the percentage error increases as the temperature function becomes more and more non-linear. There are several reasons for this. The tubular fuel assembly cannot be represented by a solid unit beam because (1) the moment of inertia is not the same (2) the cross-sectional area is not the same (3) tubes have a constant temperature in each row and cannot be represented by a continuous temperature function and (4) the tube assembly does not have isotropic characteristics.

However, before the above limitations were realized, an attempt was made to correlate the deflections computed by the solid beam theory with that of experimental results. First, the thermal stresses as a function of the co-ordinate y were plotted as shown in Figure 20. Such a plot is informative because it shows that the unit beam is in compression at the outer extremities of the beam when the temperature function is non-linear and the temperatures at each location are below that of the linear case. It would be expected that the opposite effect would result when the non-linear temperatures are above that of the linear case and such was found to be true, i.e. tension stresses resulted at the outer extremities of the distance y (see Figure 20). The strain in the axial direction, ε_x, versus y is shown to be a linear function of y in Figure 21 and if the solid beam theory were accurate for this application, a correlation would be expected to be found between ε_x and the deflection Δ. In Figure 21, the slope of each curve is observed to be somewhat proportional to the deflection, since the greatest (negative) slope corresponds to the maximum deflection for the same overall temperature difference. As the absolute value of the slope becomes less, the deflections decrease. Dividing ε_x for each curve by the deflection for that curve should yield a constant in all cases. This proved to be true when the deflection was the calculated value from solid beam theory but did not prove to be the case when the experimental deflections were used. Thus no correlation was possible between solid beam theory and experimental results.

The results of the numerical summation method are presented in Table V with the percentage error from experimental values. The deflections computed by this method employed the actual temperatures observed during the tests rather than the theoretical temperature that was desired from the temperature function. The percentage errors are small, i.e. 5% or less, and demonstrate excellent agreement. The positive percentage error may have occurred due to the inability of thermocouples to accurately record temperatures although this is doubtful. At times flow conditions were poor in some tubes due to collection of crud from the water lines and may have given a temperature reading that may not have been true. It should be pointed out here, that the moment of inertia test for determining I, differed by some 3% from that calculated. If the theoretical moment of inertia were used in the deflection and stress equation, the percentage errors would be less by 3% or essentially zero.

TABLE V

COMPARISON OF CENTER DEFLECTIONS OF REACTOR FUEL SUBASSEMBLY FROM EXPERIMENT, SOLID BEAM THEORY AND NUMERICAL SUMMATION METHOD

Temperature Function	Experimental Deflection (in.)	Solid Beam Theory (in.)	% Error	Numerical Summation Method Deflection (in.)	% Error
$T = \frac{50}{2.2}\sqrt{4.84-y^2}$	0.150	0.121	+ 19.3	0.1449	+ 3.4
$T = 50 \cos \frac{\pi}{4.4} y$	0.170	0.179	- 4.7	0.1657	+ 2.5
$T = 50 - 22.7\ y$	0.171	0.169	+ 1.1	0.1616	+ 5.5
$T = 50\ e^{-y}$	0.148	0.1407	+ 4.9	0.1397	+ 5.6
$T = 50(.25)^y$	0.156	0.142	+ 9.0	0.1479	+ 5.2
$T = 50\ e^{-2y}$	0.154	0.131	+ 15.0	0.1485	+ 3.6
$T = 50\ e^{-4y}$	0.125	0.089	+ 28.8	0.1283	- 2.6

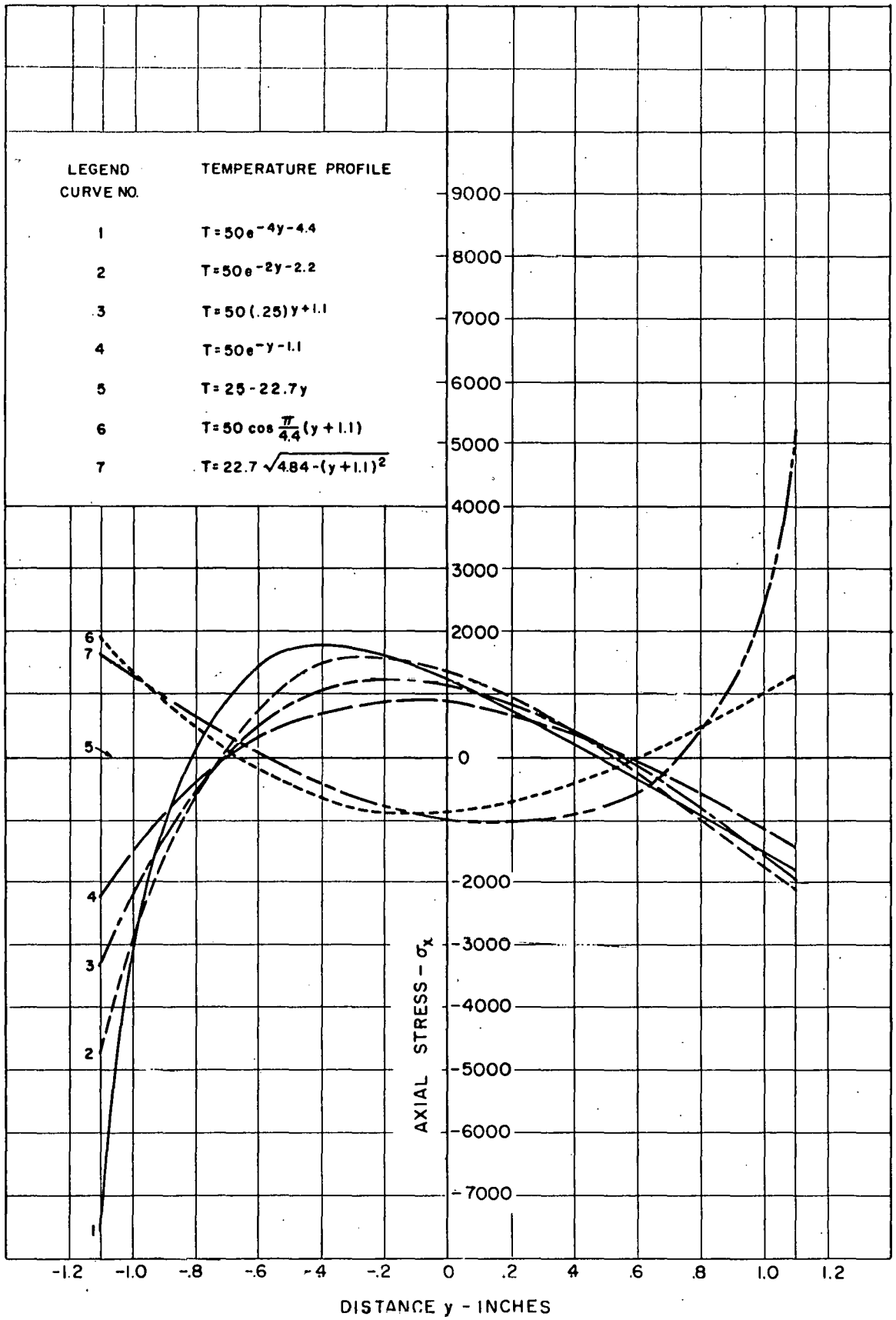

FIGURE 20

AXIAL STRESS σ_x IN PSI VERSUS DISTANCE Y FOR AN ASSUMED SOLID RECTANGULAR BEAM OF UNIT WIDTH FOR VARIOUS TEMPERATURE PROFILES ON A REACTOR SUBASSEMBLY.

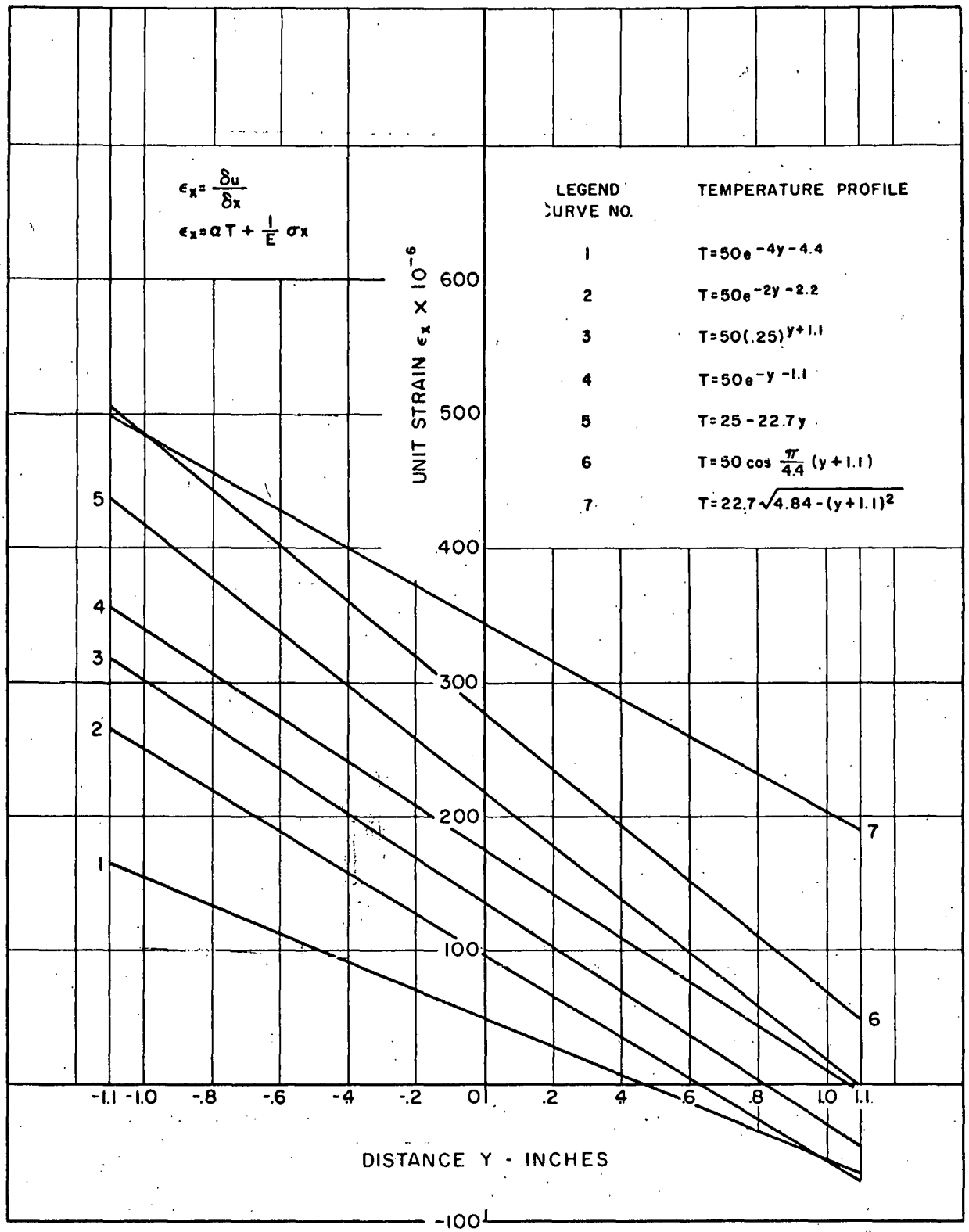

FIGURE 21

UNIT STRAIN ϵ_x VERSUS DISTANCE Y FOR VARIOUS TEMPERATURE PROFILES ON A REACTOR SUBASSEMBLY

The negative percentage error for the temperature function $T = 50\ e^{-4y}$, presents an interesting case. From Figure 20 (for the solid beam) it can be seen that for this temperature function, large compressive stresses occur on the outer tube row due to the severe thermal gradient present. It may very well be that the outer tube row buckled locally before deflecting the tube beam and this may account for the experimental deflection being less than the theoretical value. The thermal stress σ_x, at this location calculated by the numerical summation method is - 5160 psi which produces a compressive load of 107.4 pounds. The equivalent Euler buckling load for a straight axially loaded column is 497 pounds. Because the compressive load is less than the critical Euler load, it appears that buckling could not occur, but such is not the case. When the beam has a non-linear thermal gradient across it, the beam is curved, so that the critical buckling load should be considerably less since it has an eccentric load. Buckling, therefore, appears to be the only reasonable explanation of the above phenomena.

In order to apply the temperature functions shown in Figure 15 to the solid beam theory and the numerical summation method, the equations had to be rewritten so that $y = o$ at the center of the beam, consequently the axis of the temperature functions were translated by the relation $y = y' + 1.1$. This accounts for the differences shown in the temperature functions in the various figures.

It should be emphasized that the solid beam theory accurately predicts deflections for linear cases of temperature differences only because the thermal stress σ_x is zero, which means that the tubular fuel subassembly essentially acts as a solid beam for this singular specialized case. In all other non-linear cases, the solid beam theory does not predict accurate deflections.

IX. REFERENCES

1. Timoshenko, S. and Goodier, J.N., Theory of Elasticity, Second Edition, McGraw-Hill Book Co., New York, pp 399 - 416, 1951.

BIBLIOGRAPHY

1. Goodier, J.N., On the Integration of the Thermo-Elastic Equations, Philosophical Magazine and Journal of Science, Vol. 23, Seventh Series, pp. 1017-1032, Jan-June 1937.

2. Timoshenko, S., Strength of Materials, Part II, Third Edition, D. Van Nostrand Company, Inc., New York, March, 1956.

3. Dwight, B. H., Tables of Integrals and Other Mathematical Data, Third-Edition, The Macmillian Company, New York, 1957.

4. Boley, B.A., The Calculation of Thermoelastic Beam Deflection by the Principle of Virtual Work, Journal of the Aeronautical Sciences, Vol. 24, No. 1, pp 139-141, January, 1957.

5. The Reactor Handbook - Engineering, Volume 2 United States Atomic Energy Commission May, 1955, AECD-3646.

6. Born, J.S. and Horvay, G., "Thermal Stresses in Rectangular Strips - II", The American Society of Mechanical Engineers, National Conference of the Applied Mechanics Division, Troy, N.Y., June 16-18, 1955.

7. Giedt, W. H., Principles of Engineering Heat Transfer, D. Van Nostrand Company, Inc. New York, August, 1957.

8. Johnson, C. G., Thermal Deflection of a Reactor Fuel Assembly From Linear and Non-Linear Temperature Gradients. An M.S. Thesis submitted to the University of Pittsburgh in partial fulfillment of the requirements for the degree Master of Science, December, 1958.

ACKNOWLEDGEMENTS

The author wishes to express his appreciation to E. A. Davis of the Westinghouse Research Laboratories and R. J. Erdlac of the University of Pittsburgh for their able assistance and helpful criticism. Mr. A. G. Thorp II and R. Heatherington of the Westinghouse Atomic Power Department contributed much of their valuable time in providing many helpful suggestions and assisting with experimental problems.

The author is indebted to the Nuclear Design Section of the WAPD Reactor Engineering Department for providing the necessary nuclear parts for the analysis of thermal deflection in this report.

APPENDIX A

Sample Calculation of Linear Temperature Difference

Total Heat Output $Q = 392 \text{ MW} \times 10^3 \frac{\text{KW}}{\text{MW}} \times 3413 \frac{\text{Btu}}{\text{KW-HR}} = 1338 \times 10^6 \text{ Btu/hr}$

at a Radius of 11.5 inches (at hot channel location)

$$\bar{Q} = \frac{1338 \times 10^6}{23{,}218} = 57{,}700 \text{ Btu/hr-rod}$$

$$\bar{Q}_{R_1} = 57{,}700 \times \frac{0.585}{0.350} = 96{,}500 \text{ Btu/hr-rod}$$

For the temperature rise of water

$$Q_x = W \, Cp \, \Delta T_{w_x} \qquad \text{where } W = \frac{\text{Coolant Flow}}{\text{Total No. of Rods}}$$

$$\Delta T_{w_x} = \frac{Q_x}{W \, Cp} \qquad W = \frac{34.0 \times 10^6}{23{,}218} = 1464 \text{ lbs/hr-rod}$$

$$\Delta T_{w_x} = \frac{Q_x}{1464 \, Cp} \qquad \text{where } Cp = 1.205 \text{ Btu/lb-}^\circ\text{F at } 530^\circ\text{F}$$

$$Cp_{H.C.} = 1.278 \text{ Btu/lb-}^\circ\text{F at } 560^\circ\text{F}$$

For Hot Channel

$$\Delta T_{w_{xH.C.}} = F_{\Delta T} \cdot \Delta T_{w_x} = 1.392 \ \Delta T_{w_x}$$

Applying flux peaking factor

$$\Delta T_{w_{xH.C.}} = F_{fp} \cdot F_{\Delta T} \cdot \Delta T_{w_x} = 1.20 \times 1.392 \ \Delta T_{w_x} = 1.67 \ \Delta T_{w_x}$$

$$\therefore T_{w_x} = T_{in} + \Delta T_{w_{xH.C.}} = 499.5 + 1.67 \ \Delta T_{w_x}$$

For The Film Temperature Rise

$$Q_x = h_F \, A_S \, \theta_F \qquad \text{where } h_F = 6050 \text{ Btu/hr-ft}^2\text{-}^\circ\text{F}$$

$$\theta_F = \frac{Q_x}{h_F \, A_S} = \frac{Q_x}{223} \qquad A_s = 0.0368 \text{ Ft}^2 \text{ for each } 5'' \text{ increment along rod of } 0.337 \text{ O.D.}$$

For Hot Channel

$$\theta_{F_{H.C.}} = F \cdot \theta_F = 1.532 \ \theta_F$$

Applying Flux Peaking Factor

$$\theta_{F_{H.C.}} = F_{fp} \cdot F_{\theta} \cdot \theta_F = 1.20 \times 1.532\ \theta_F = 1.84\ \theta_F$$

$$\therefore T_{s_x} = T_{w_x} + 1.84\ \theta_{F_x}$$

For Tube (clad) Temperature Rise

$$\Delta T_c = \frac{Q_x\ \ell n \frac{b_1}{a_1}}{2\pi\ KL} \qquad \text{where } \frac{b_1}{a_1} = \frac{0.1685}{0.1475} = 1.142$$

$$\Delta T_c = 0.00486\ Q_x \qquad K = 10.6 \text{ Btu/hr-ft}^2\text{-}^{\circ}\text{F-ft}$$

$$L = 5/12 \text{ ft.}$$

For Hot Channel

$$\Delta T_{c_{H.C.}} = F_q\ \Delta T_c = 1.078\ \Delta T_c$$

$$Tc_{x_{H.C.}} = T_{S_x} + \frac{1.078\ \Delta T_c}{2}$$

At a radius of 15.25 inches (at Avg. Channel Location)

$$\overline{Q}_{R_2} = 57{,}700 \times \frac{0.540}{0.350} = 89000 \text{ Btu/hr-rod}$$

For the temperature rise of the water

$$T_{w_x} = 499.5 + \Delta T_{w_x}$$

For the film temperature rise

$$T_{S_x} = T_{w_x} + \theta_{F_x}$$

For the tube (clad) temperature rise

$$T_{c_x} = T_{S_x} + \frac{\Delta T_c}{2}$$

Note: The results are presented in Tables A-I and A-II.

APPENDIX A

TABLE A-I

HOT CHANNEL AT 11.5 INCHES RADIUS

Distance From Inlet (in.)	% Heat Given Off	Q_{R_1} Btu/hr.	ΔT_{W_X} °F	$\Delta T_{W_{X_{H.C.}}}$ °F	T_{W_X} °F	θ_{F_X} °F	$\theta_{F_{H.C.}}$ °F	T_S °F	$\Delta T_{c_{H.C.}}$ °F	$T_{c_{X_{H.C.}}}$ °F *
5	4.07	3930	2.10	3.50	503.00	17.6	32.4	535.40	20.3	545.5
10	5.76	5560	2.97	4.96	507.96	24.9	45.9	553.86	28.6	568.2
15	7.75	7475	3.99	6.67	514.63	33.5	61.7	576.33	38.5	595.6
20	9.40	9060	4.84	8.09	522.72	40.6	74.8	597.52	46.7	620.8
25	10.55	10190	5.44	9.08	531.80	45.7	84.0	615.80	52.4	642.0
30	11.07	10600	5.70	9.52	541.32	47.9	88.1	629.42	55.0	656.9
35	11.02	10630	5.68	9.49	550.81	47.7	87.7	638.51	54.8	665.9
40	10.35	100000	5.34	8.90	559.71	44.8	82.5	642.21	51.5	668.0
45	9.13	8800	4.70	7.85	567.56	39.5	72.6	640.16	45.3	662.8
50	7.40	7140	3.81	6.37	573.93	32.0	58.9	632.83	37.8	646.2
55	5.13	4950	2.64	4.41	578.34	22.2	40.8	619.14	25.5	631.8
60	3.20	3090	1.65	2.76	581.10	13.85	25.5	606.60	15.9	614.5
65	1.98	1910	1.02	1.70	582.80	8.56	15.8	598.60	9.8	603.5
70	1.29	1244	0.665	1.11	583.91	5.58	10.3	594.21	6.4	597.4
75	0.83	800	0.427	0.71	584.62	3.59	6.6	591.22	4.1	593.3
80	0.53	511	0.273	0.46	585.08	2.29	4.4	589.48	2.6	590.8
85	0.33	318	0.170	0.28	585.36	1.43	2.6	587.96	1.6	588.8
90	0.21	202	0.108	0.18	585.64	0.91	1.7	586.34	1.0	586.8

* These temperatures are plotted in Figure 6.

APPENDIX A

TABLE A-11

AVERAGE CHANNEL AT 15.25 INCHES RADIUS

Distance From Inlet (in)	% Heat Given Off	Q_{R_2} Btu/hr.	ΔT_{W_x} °F	T_{W_x} °F	θ_{F_x} °F	T_S °F	ΔT_c °F	T_c °F *
5	4.07	3630	2.05	501.55	15.8	517.4	17.7	526.2
10	5.76	5130	2.91	504.46	23.0	527.5	25.1	540.0
15	7.75	6900	3.91	508.37	30.9	539.3	33.7	556.1
20	9.40	8360	4.74	513.11	37.5	550.6	40.8	571.0
25	10.55	9400	5.32	518.43	42.1	560.5	45.9	583.4
30	11.07	9860	5.59	524.02	44.2	568.2	48.2	592.3
35	11.02	9810	5.56	529.58	44.0	573.6	47.9	597.6
40	10.35	9210	5.22	534.80	41.3	576.1	45.0	598.6
45	9.13	8120	4.60	539.40	36.4	575.8	39.6	595.6
50	7.40	6590	3.74	543.14	29.5	572.6	32.2	588.7
55	5.13	4560	2.58	545.72	20.4	566.1	22.3	577.3
60	3.20	2850	1.62	547.34	12.8	560.1	13.9	567.0
65	1.98	1760	1.00	548.34	7.9	556.2	8.6	560.5
70	1.29	1150	0.652	548.99	5.2	554.2	5.6	557.0
75	0.83	740	0.420	549.41	3.3	552.7	3.6	554.5
80	0.53	472	0.268	549.68	2.1	551.8	2.3	553.0
85	0.33	294	0.166	549.85	1.3	551.1	1.4	551.8
90	0.21	187	0.106	549.96	0.8	550.8	0.9	551.2

* These temperatures are plotted in Figure 5

APPENDIX B

Deflection by Solid Beam Method

Temperature Function $T = 50\, e^{-4y-4.4}$

The Stress Equation is

$$\sigma_x = -\alpha E \cdot T(y) + \frac{1}{2c}\int_{-c}^{+c} \alpha E \cdot T(y)\, dy + \frac{3y}{2c^3}\int_{-c}^{+c} \alpha E \cdot T(y) \cdot y\, dy$$

$$\sigma_x = -\alpha E\,(50\, e^{-4y-4.4}) + \frac{1}{2c}\int_{-c}^{+c} \alpha E(50\, e^{-4y-4.4})dy + \frac{3y}{2c^3}\int_{-c}^{+c} \alpha E\,(50\, e^{-4y-4.4})ydy$$

Let $X = -4y-4.4$ and $-4y = x + 4.4$

$dx = -4dy$ $\qquad y = \dfrac{x + 4.4}{-4}$

$-1/4\, dx = dy$

Change Limits of Integration - When

$y = +c = +1.1$ $\qquad x = -4\,(1.1) - 4.4 = -8.8$

$y = -c = -1.1$ $\qquad x = -4\,(-1.1) - 4.4 = 0$

Also $A \alpha E = 50 \times 8.7 \times 10^{-6} \times 28 \times 10^{6} = 12{,}200$

$$\sigma_x = -12{,}200\, e^{-4y-4.4} + \frac{12{,}200}{2\,(1.1)}\int_{0}^{-8.8} e^{x}\left(-\frac{1}{4}\, dx\right) + \frac{3y(12{,}200)}{2\,(1.1)^3}\int_{0}^{-8.8} e^{x}\left(\frac{x + 4.4}{-4}\right)\left(\frac{dx}{-4}\right)$$

$$\sigma_x = -12{,}200\, e^{-4y-4.4} - 1390\left[e^{-8.8} - e^{0}\right] + 860\, y\left[e^{-8.8}(-8.8-1+4.4) - (-1+4.4)\right]$$

$$\sigma_x = -12{,}200\, e^{-4y-4.4} + 1390 - 2920\, y$$

The strains are

$$\varepsilon_x - \alpha \cdot T(y) = \frac{1}{E}\,\sigma_x \qquad \text{Since } \sigma_y = 0,\ \sigma_z = 0$$

$$\varepsilon_y - \alpha \cdot T(y) = \frac{\nu}{E}\,\sigma_x$$

Substituting in the Stress σ_x

$$E\,\varepsilon_x = E\,\alpha\,(50\, e^{-4y-4.4}) + (-12200\, e^{-4y-4.4} + 1390 - 2920y)$$

$$E\,\varepsilon_y = E\,\alpha\,(50\, e^{-4y-4.4}) - \nu\,(-12200\, e^{-4y-4.4} + 1390 - 2920y)$$

which becomes

$$E\,\varepsilon_x = E\,\frac{\partial u}{\partial x} = +1390 - 2920\,y$$

$$E\,\varepsilon_y = E\,\frac{\partial v}{\partial y} = \left[12200\,(1+\nu)\right] e^{-4y-4.4} - 1390\nu + 2920\,\nu y$$

Let $D = \left[12200\,(1+\nu)\right]$

Then

$$Eu = 1390x - 2920\,xy + f(y)$$

$$Ev = \frac{De^{-4y-4.4}}{-4} - 1390\,\nu y + 2920\,\frac{\nu y^2}{2} + f(x)$$

$$\gamma_{xy} = \frac{\partial u}{\partial y} + \frac{\partial v}{\partial x} = \frac{\tau_{xy}}{G} = 0$$

$$\therefore\ \frac{1}{E}\left(-2920x + \frac{\partial f(y)}{\partial y}\right) + \frac{1}{E}\,\frac{\partial f(x)}{x} = 0$$

or

$$-2920x + \frac{\partial f(y)}{\partial y} + \frac{\partial f(x)}{\partial x} = 0$$

From above, let

$$F(x) = -2920x + \frac{\partial f(x)}{\partial x}, \quad G(y) = \frac{\partial f(y)}{\partial y}, \quad K = 0$$

Let

$$F(x) = d,\ G(y) = \bar{e}$$

Then we obtain

$$F(x) + G(y) = K$$

$$\therefore\ d + \bar{e} = 0$$

$$\frac{\partial f(x)}{\partial x} = +2920\,x + d, \quad \frac{\partial f(y)}{\partial y} = \bar{e}$$

Upon integration, the unknown functions become

$$f(x) = 2920 \frac{x^2}{2} + dx + g$$

$$f(y) = \bar{e}\, y + h$$

The displacements become

$$Eu = 1390\, x - 2920\, xy + \bar{e}\, y + h$$

$$Ev = \frac{De^{-4y} - 4.4}{-4} - 1390\, \nu y + 2920 \frac{\nu y^2}{2} + 2920 \frac{x^2}{2} + dx + g$$

Applying Boundary Conditions

1st B.C. at $x = 0$, $y = 0$ Let $u = 0$ $\therefore$ $h = 0$

2nd B.C. at $x = 0$, $y = 0$ Let $\frac{v}{x} = 0$ $\therefore$ $d = 0$

3rd B.C. If $d = 0$ $\bar{e} + d = 0$ $\therefore$ $\bar{e} = 0$

4th B.C. At $x = \pm L$, $y = 0$ Let $v = 0$ $g = \frac{De^{-4.4}}{4} - 2920 \frac{L^2}{2}$

The Displacements are

$$Eu = 1390\, x - 2920\, xy$$

$$Ev = \frac{De^{-4y-4.4}}{-4} - 1390\, \nu y + 2920 \frac{\nu y^2}{2} + 2920 \frac{x^2}{2} + \frac{De^{-4.4}}{4} - 2920 \frac{L^2}{2}$$

The Deflection curve is obtained by substituting $y = 0$ into the equation for v.

$$E\Delta = \frac{De^{-4.4}}{-4} + 2920 \frac{x^2}{2} + \frac{De^{-4.4}}{4} - 2920 \frac{L^2}{2}$$

and when $x = 0$ $v = \Delta_{max}$

$$E\Delta_{max} = -2920 \frac{L^2}{2}$$

$$\Delta_{max} = -\frac{2920\, L^2}{2E}$$

For the Beam Under Consideration

$$\Delta_{max} = - \frac{2920\ L^2}{2E} = \frac{-2920\ (41.5)^2}{2 \times 28 \times 10^6}$$

$$\Delta_{max} = - 0.0899" \quad (28\% \text{ Error})$$

Actual Experimental Deflection = - 0.125"

APPENDIX C

Deflection by Numerical Summation Method

Temperature Function $T = 50\, e^{-4y-4.4}$

Distance y, in.	- 1.1	- 0.66	- 0.22	+ 0.22	+ 0.66	+ 1.1
Temperature T, °F	50	8.6	2	0	0	0

The Stress Equation is

$$\sigma_x = - \alpha E \cdot T(y) + \frac{1}{A} \sum_{1}^{N} \alpha E \cdot T_N \cdot A_N + \frac{y}{I} \sum_{1}^{N} \alpha E \cdot T_N \cdot y_N \cdot A_N$$

The equation can be rewritten

$$\sigma_x = - \alpha E\, (50\, e^{-4y-4.4}) + b + cy$$

where

$$b = \frac{1}{A} \sum_{1}^{N} \alpha E \cdot T_N \cdot A_N = \frac{8.7 \times 10^{-6} \times 28 \times 10^{+6}}{0.750} \left[0.125\ (50+8.6+2+0+0+0)\right] = 2460$$

$$c = \frac{1}{I} \sum_{1}^{N} \alpha E \cdot T_N \cdot y_N \cdot A_N = \frac{8.7 \times 10^{-6} \times 28 \times 10^{+6}}{0.446} \left[0.125\left\{50(-1.1)+8.6(-.66)+2(-.22)\right\}\right.$$

$$c = -4172$$

The Stress Equation for this step function is:

$$\sigma_x = - 12{,}200\, e^{-4y-4.4} + 2460 - 4172\, y$$

The Strains are

$$\varepsilon_x - \alpha \cdot T(y) = \frac{1}{E} \sigma_x \qquad \text{Since } \sigma_y = 0,\ \sigma_Z = 0$$

$$\varepsilon_y - \alpha \cdot T(y) = \frac{\nu}{E} \sigma_x$$

Substituting in the Stress σ_x

$$E\,\varepsilon_x = E\,\alpha\,(50\,e^{-4y-4.4}) + (-12{,}200\,e^{-4y-4.4} + 2460 - 4172y)$$

$$E\,\varepsilon_y = E\,\alpha\,(50\,e^{-4y-4.4}) - \nu\,(-12{,}200\,e^{-4y-4.4} + 2460 - 4172\,y)$$

which becomes

$$E\,\varepsilon_x = E\,\frac{\partial u}{\partial x} = 2460 - 4172\,y$$

$$E\,\varepsilon_y = E\,\frac{\partial v}{\partial y} = \left[12{,}200\,(1 + \nu)\right]\,e^{-4y-4.4} - 2640\nu + 4172\,\nu y$$

Let $D = \left[12{,}200\,(1 + \nu)\right]$

Then

$$E\,u = 2460\,x - 4172\,xy + f(y)$$

$$E\,v = \frac{De^{-4y-4.4}}{-4} - 2460\,\nu y + 4172\,\frac{\nu y^2}{2} + f(x)$$

$$\gamma_{xy} = \frac{u}{y} + \frac{v}{x} = \frac{\tau_{xy}}{G} = 0$$

$$\therefore \frac{1}{E}\,(-4172\,x + \frac{\partial f(y)}{\partial y}) + \frac{1}{E}\,(\frac{\partial f(x)}{\partial x}) = 0$$

or $$-4172\,x + \frac{\partial f(y)}{\partial y} + \frac{\partial f(x)}{\partial x} = 0$$

From above, Let

$$F(x) = -4172\,x + \frac{\partial f(x)}{\partial x}, \quad G(y) = \frac{\partial f(y)}{\partial y}, \quad K = 0$$

Let

$$F(x) = d, \quad G(y) = \bar{e}$$

Then we obtain

$$F(x) + G(y) = K$$

$$\therefore \quad d + \bar{e} = 0$$

$$\frac{\partial f(x)}{\partial x} = 4172\,x + d, \qquad \frac{\partial f(y)}{\partial y} = \bar{e}$$

Upon integration, the unknown functions become

$$f(x) = 4172 \frac{x^2}{2} + dx + g$$

$$f(y) = \bar{e}\, y + h$$

The displacements become

$$E\,u = 2460\,x - 4172\,xy + \bar{e}y + h$$

$$E\,v = \frac{De^{-4y-4.4}}{-4} - 2460\,\nu y + 4172\,\frac{\nu y^2}{2} + 4172\,\frac{x^2}{2} + dx + g$$

Applying Boundary Conditions

1st B.C. at $x = 0,\ y = 0$ Let $u = 0$ $\therefore h = 0$

2nd B.C. at $x = 0,\ y = 0$ Let $\frac{\nu}{x} = 0$ $\therefore d = 0$

3rd B.C. if $d = 0$, $\bar{e} + d = 0$ $\therefore \bar{e} = 0$

4th B.C. at $x = \pm L,\ y = 0$ Let $v = 0$ $g = \frac{De^{-4.4}}{4} - 4172\,\frac{L^2}{2}$

The displacements are

$$E\,u = \left[2460\,x - 4172\,xy\right]$$

$$E\,v = \frac{De^{-4y-4.4}}{-4} - 2460\,\nu y + 4172\,\frac{\nu y^2}{2} + 4172\,\frac{x^2}{2} + \frac{De^{-4.4}}{4} - 4172\,\frac{L^2}{2}$$

The Deflection curve is obtained by substituting $y = 0$ into the equation for v.

$$E\Delta = \frac{De^{-4.4}}{-4} + 4172\,\frac{x^2}{2} + \frac{De^{-4.4}}{4} - 4172\,\frac{L^2}{2}$$

and when $x = 0$ $v = \Delta_{max}$

$$\Delta_{max} = \frac{-4172\,(L^2)}{2E} = -\frac{4172\,(41.5^2)}{2 \times 28 \times 10^6}$$

$$\Delta_{max} = 0.1283" \text{ (-2.6\% error)}$$

Actual experimental deflection = - 0.125"